Electron Interactions With c-C_4F_8

L. G. Christophorou[a] and J. K. Olthoff[b]

Electricity Division, Electronics and Electrical Engineering Laboratory, National Institute of Standards and Technology, Gaithersburg, Maryland 20899-8113

The limited electron collision cross-section and transport-coefficient data for the plasma processing gas perfluorocyclobutane (c-C_4F_8) are synthesized, assessed, and discussed. These include cross sections for total electron scattering, differential elastic electron scattering, partial and total ionization, dissociation into neutral fragments, and electron attachment, as well as data on electron transport, ionization, and attachment coefficients. The available data on both the electron collision cross sections and the electron transport coefficients require confirmation. Also, measurements are needed of the momentum transfer and elastic integral cross sections, and of the cross sections for other significant low-energy electron collision processes such as vibrational and electronic excitation. In addition, electron transport data over a wider range of values of the density-reduced electric field are needed. The present assessment of data on electron affinity, attachment, and scattering suggests the existence of negative ion states near -0.6, 4.9, 6.9, 9.0, and 10.5 eV. © *2001 by the U.S. Secretary of Commerce on behalf of the United States. All rights reserved.*

Contents

List of Tables

[a]Electronic mail: loucas.christophorou@nist.gov
[b]Electronic mail: james.olthoff@nist.gov

List of Figures

1. Introduction

Perfluorocyclobutane (c-C_4F_8) is a processing gas employed in plasma etching (e.g., see Refs. 1–7). Electron impact on c-C_4F_8 generates large quantities of CF_2 radicals, which in c-C_4F_8 plasmas form a polymer coating on silicon and account for the high etching selectivity of SiO_2 over Si by c-C_4F_8 plasmas.[3,5–7] The c-C_4F_8 molecule also decomposes thermally above about 633 K,[8] principally via the unimolecular decomposition reaction c-$C_4F_8\rightarrow2\,C_2F_4$ (see Refs. 8, 9 and references cited therein), and thus CF_2 radicals may also be formed in a c-C_4F_8 plasma by electron-impact dissociation of the C_2F_4 byproduct. Consistent with this decomposition mechanism are infrared multiphoton dissociation studies[10–13] of c-C_4F_8 which show that photodissociation occurs via the process c-$C_4F_8+nh\nu\rightarrow2\,C_2F_4$.

Besides its use in plasma etching, c-C_4F_8 has many other applications ranging from its use in retinal detachment surgery,[14,15] to its possible utilization as a gaseous dielectric especially in gas mixtures.[16–19] Perfluorocyclobutane is also of environmental interest because it is a global warming gas.[20] Its lifetime in the atmosphere, based on the assumption that photolysis is the dominant atmospheric loss process for c-C_4F_8, is very long (3200 yr).[20] However, Morris et al.[21] argue that the atmospheric lifetime of c-C_4F_8 is significantly reduced (to 1400 yr) if consideration is given to its atmospheric removal by electron interactions. The long atmospheric lifetime of c-C_4F_8 partly accounts for its high global warming potential, which over a 100-yr time period is 8700 times that of CO_2.[20]

In this paper a number of collision cross sections, coefficients, and rate constants are used to quantify the various processes which result from collisions of low-energy (mostly less than 100 eV) electrons with the c-C_4F_8 molecule. These physical quantities are identified in Table 1 along with the

corresponding symbols and units. The procedure for assessing and recommending data followed in this paper is the same as in the previous nine papers in this series.[22–30] Few of the available data sufficiently meet the assessment criteria[22,25] to be ''recommended,'' but suggested data are presented where possible. There is a need for further measurements on most of the electron collision cross sections and coefficients.

Besides the experimental data summarized, assessed, and discussed in this paper, there has been no published review and/or assessment of the data on the electron collision cross sections and electron transport coefficients for this molecule. There have been however two Boltzmann-code calculations[31,32] of various coefficients, but these results are not discussed in this paper due to their unknown uncertainty.

2. Structural and Electronic Properties

Electron diffraction studies[33–38] have shown that the carbon atoms in the c-C_4F_8 molecule are not planar. Similarly, infrared studies[39–42] are consistent with a nonplanar molecular structure. The c-C_4F_8 molecule has a puckered structure and belongs to the D_{2d} symmetry point group. Table 2 lists information on its structural properties and also values of the electron affinity, ionization threshold energy, dissociation energy, and polarizability of the c-C_4F_8 molecule.

The c-C_4F_8 molecule forms parent negative ions below ~ 1 eV and this property is consistent with the molecule having a positive electron affinity (EA). Besides the ''zero-energy'' electron attachment process which is associated with the negative ion state located at –EA, fragment negative ions are formed via a number of negative ion states which lie between 0 and ~ 12 eV. The energy positions of these negative ion states as indicated by the experimental data on negative ion formation are listed in Table 3 and plotted in Fig. 1. The similar results obtained from electron scattering experiments are also listed in Table 3 and plotted in Fig. 1. In the last column of Fig. 1 are shown the suggested energy positions of the lowest negative ion states of c-C_4F_8: -0.62, 4.9, 6.9, 9.0, and 10.5 eV. These suggested values were determined as follows: The value -0.62 eV is the average of the highest two electron affinity values listed in Table 2. The third (lower) value was not considered since it is only a lower limit. The 4.9 and 9.0 eV values are those from electron scattering experiments, which are expected to lie somewhat higher than the corresponding values determined from dissociative electron attachment experiments. The 6.9 and the 10.5 eV values are averages of values measured by various groups (see Table 3) for the energies at which the cross section for F^- production by electron attachment exhibits a maximum.

3. Electron Scattering Cross Sections

3.1. Total electron scattering cross section, $\sigma_{\text{sc,t}}(\varepsilon)$

There have been two recent measurements[57–59] of the total electron scattering cross section $\sigma_{\text{sc,t}}(\varepsilon)$ of c-C_4F_8 which are compared in Fig. 2. The measurements of Sanabia et al.[57] cover the low-energy range from 1 to 20 eV and those of Nishimura[58,59] cover a wider energy range from 2 to 3000 eV. Sanabia et al. did not quote the uncertainty of their data, but Nishimura gives the combined systematic and statistical uncertainties of his measurements to be between 2.8% and 5.9% depending on the electron energy. Representative error bars for the data of Nishimura are shown in Fig. 2. Generally, the data of Nishimura lie higher than those of Sanabia et al.[57]

TABLE 1. Definition of symbols

Symbol	Definition	Common scale and units
$\sigma_{\text{sc,t}}(\varepsilon)$	Total electron scattering cross section	10^{-16} cm^2; 10^{-20} m^2
$\sigma_{\text{e,diff}}$	Elastic differential electron scattering cross section	10^{-16} cm^2 sr^{-1}
$\sigma_{\text{vib,diff}}(\varepsilon)$	Vibrational differential electron scattering cross section	10^{-16} cm^2 sr^{-1}
$\sigma_{\text{i,partial}}(\varepsilon)$	Partial ionization cross section	10^{-16} cm^2; 10^{-20} m^2
$\sigma_{\text{i,t}}(\varepsilon)$	Total ionization cross section	10^{-16} cm^2; 10^{-20} m^2
$\sigma_{\text{dis,partial}}(\varepsilon)$	Partial cross section for dissociation into neutrals	10^{-18} cm^2; 10^{-22} m^2
$\sigma_{\text{a,t}}(\varepsilon)$	Total electron attachment cross section	10^{-15} cm^2; 10^{-19} m^2
$\sigma_{\text{da,t}}(\varepsilon)$	Total dissociative electron attachment cross section	10^{-16} cm^2; 10^{-20} m^2
$\alpha/N\,(E/N)$	Density-reduced ionization coefficient	10^{-18} cm^2 or 10^{-22} m^2
$(\alpha-\eta)/N\,(E/N)$	Density-reduced effective ionization coefficient	10^{-18} cm^2 or 10^{-22} m^2
$k_{\text{a,t}}\,(E/N)$	Total electron attachment rate constant	10^{-9} cm^3 s^{-1}
$(k_{\text{a,t}})_{\text{th}}$	Thermal electron attachment rate constant	10^{-9} cm^3 s^{-1}
$\eta/N\,(E/N)$	Density-reduced electron attachment coefficient	10^{-17} cm^2 or 10^{-21} m^2
$w\,(E/N)$	Electron drift velocity	10^7 cm s^{-1}
$D_{\text{T}}/\mu\,(E/N)$	Ratio of lateral electron diffusion coefficient to electron mobility	V

TABLE 2. Physical and structural data on the c-C_4F_8 molecule

Physical quantity	Value	Reference	Method
Electron affinity	~0.63 eV	43	Electron attachment/detachment studies
	0.61 eV	44	Electron attachment
	≥0.4 eV	45	Endothermic negative-ion charge-transfer reactions
Ionization threshold energy	11.6±0.2 eV	46	TPEPICO[a] spectroscopy
	12.1±0.1 eV[b]	47	Electron impact
	12.23 eV[c]	48	
	12.25 eV[d]	49	Electron impact
Dissociation energy, D(C–F)	~4.4±0.2 eV	47	Electron impact
Polarizability	73.7×10^{-25} cm^3	50	From data on liquid density and refractive index using the Lorenz–Lorentz equation.
	92.4×10^{-25} cm^3	50	Using ion cyclotron resonance data
	74.9×10^{-25} cm^3	50	Semiempirical calculation
	104.3×10^{-25} cm^3	50	Semiempirical calculation
	124.7×10^{-25} cm^3	50	Semiempirical calculation
Molecular structure[e] parameters			
C–C internuclear distance	1.63±0.02 Å	35	Electron diffraction
	1.60±0.04 Å	34	Electron diffraction
	1.58 Å	38	Electron diffraction
	1.566±0.008 Å	36	Electron diffraction
	1.560±0.009 Å	37	Electron diffraction
	1.54 Å	33	Electron diffraction
C–F internuclear distance	1.38 Å	33	Electron diffraction
	1.333±0.002 Å	36	Electron diffraction
	1.333 Å	38	Electron diffraction
	1.332±0.005 Å	35	Electron diffraction
	1.33±0.02 Å	34	Electron diffraction
	1.324±0.005 Å	37	Electron diffraction
F–C–F angle	110°	38	Electron diffraction
	109.9°±0.3°	36	Electron diffraction
	109.5°±3°	34	Electron diffraction
	109°±1°	37	Electron diffraction
	108°±2°	35	Electron diffraction
C–C–C angle	89.3°±0.3°	36	Electron diffraction
	~89°	34	Electron diffraction
	88.8°	38	Electron diffraction
Dihedral angle	10°±3°	35	Electron diffraction
	17.4°±0.3°	36	Electron diffraction

[a]Threshold photoelectron–photoion coincidence technique.
[b]This is the value of the threshold energy for the formation of $C_3F_5^+$, the lowest threshold value for the positive ions listed in Ref. 47.
[c]Vertical value.
[d]The same (lowest) value is listed for the ''appearance'' of $C_3F_5^+$ and $C_2F_4^+$.
[e]Chang *et al.*[36] give the tilt angle for CF_2 to be −5.4°.

TABLE 3. Negative ion states of c-C_4F_8

Energy position (eV)	Type of measurement	Reference
~ 0.0	Nondissociative electron attachment	51
0.03^a $(0.23)^b$	Nondissociative electron attachment	52, 47
0.4 ± 0.08	Total electron attachment	53
0.45 ± 0.1	Nondissociative electron attachment	54
1.75^a $(1.9)^b$	Dissociative electron attachment producing F^-	47
1.75^a $(1.9)^b$	Dissociative electron attachment producing $C_3F_5^-$	47
3.75^a $(4.05)^b$	Dissociative electron attachment producing $C_3F_5^-$	47
4.1	Dissociative electron attachment producing $C_3F_5^-$	51
4.3	Dissociative electron attachment producing F^-	49
4.3^a $(4.6)^b$	Dissociative electron attachment producing F^-	47
4.35^a	Dissociative electron attachment producing CF_3^-	47
4.35 ± 0.1	Dissociative electron attachment producing $C_2F_5^-$	54
4.4^a	Dissociative electron attachment producing $C_2F_5^-$	47
4.5 ± 0.08	Dissociative electron attachment producing F^-	53
4.8	Dissociative electron attachment producing F^-	51
4.8	Dissociative electron attachment producing CF_3^-	51
4.9	Dissociative electron attachment producing $C_2F_3^-$	51
4.95 ± 0.1	Dissociative electron attachment producing F^-	54, 55
4.95 ± 0.1	Dissociative electron attachment producing F_2^-	54
4.95 ± 0.1	Dissociative electron attachment producing CF_2^-	54
4.95 ± 0.1	Dissociative electron attachment producing CF_3^-	54, 55
5.0	Dissociative electron attachment producing CF_3^-	49
4.91	Derivative electron transmission spectrum	56
~ 6	Total electron scattering cross section	57
6.5	Dissociative electron attachment producing F^-	51
6.75^a $(7.1)^b$	Dissociative electron attachment producing F^-	47
6.8	Dissociative electron attachment producing F^-	49
6.9 ± 0.08	Dissociative electron attachment producing F^-	53
7.4 ± 0.2	Dissociative electron attachment producing F^-	54, 55
7.9	Dissociative electron attachment producing F^-	51
7.9	Dissociative electron attachment producing $C_2F_3^-$	51
8.0	Dissociative electron attachment producing F^-	49
8.1 ± 0.08	Dissociative electron attachment producing F^-	53
8.2^a $(8.45)^b$	Dissociative electron attachment producing F^-	47
8.5 ± 0.3	Dissociative electron attachment producing F_2^-	54
8.6 ± 0.2	Dissociative electron attachment producing F^-	54, 55
8.8 ± 0.1	Dissociative electron attachment producing CF_2^-	54
~ 9	Total electron scattering cross section	58, 59
~ 9	Total electron scattering cross section	57
10.2	Dissociative electron attachment producing F^-	51
10.3	Dissociative electron attachment producing F^-	49
10.4 ± 0.08	Dissociative electron attachment producing F^-	53
10.4 ± 0.3	Dissociative electron attachment producing F_2^-	54
10.5^a $(10.8)^b$	Dissociative electron attachment producing F^-	47
10.8 ± 0.2	Dissociative electron attachment producing F^-	54, 55
11.2 ± 0.2	Dissociative electron attachment producing CF_2^-	54

^{a}Calibration made using the production of SF_6^- from SF_6 (peak at 0.0 eV).
^{b}Calibration made using the production of O^- from CO (peak at 9.8 eV).

The cross section of Sanabia *et al.*[57] shows a pronounced minimum at ~ 4 eV and it rises steeply as the energy is decreased below ~ 2 eV. This latter feature is consistent with a large electron attachment cross section near zero energy (see Sec. 6.4). The cross section of Sanabia *et al.* also indicates a minor enhancement near 6.0 eV, which is consistent with the existence of a negative ion resonance at 5.9 eV, as detected in the derivative electron transmission spectrum[56] and in dissociative electron attachment studies near 5 eV (see Table 3). Both the cross section data of Sanabia *et al.* and Nishimura *et al.*[58,59] show another cross section enhancement near 9 eV, which is in agreement with dissociative electron attachment studies indicating (see Table 3) a negative ion state at this energy. In addition, the data of Nishimura show ''humps'' at
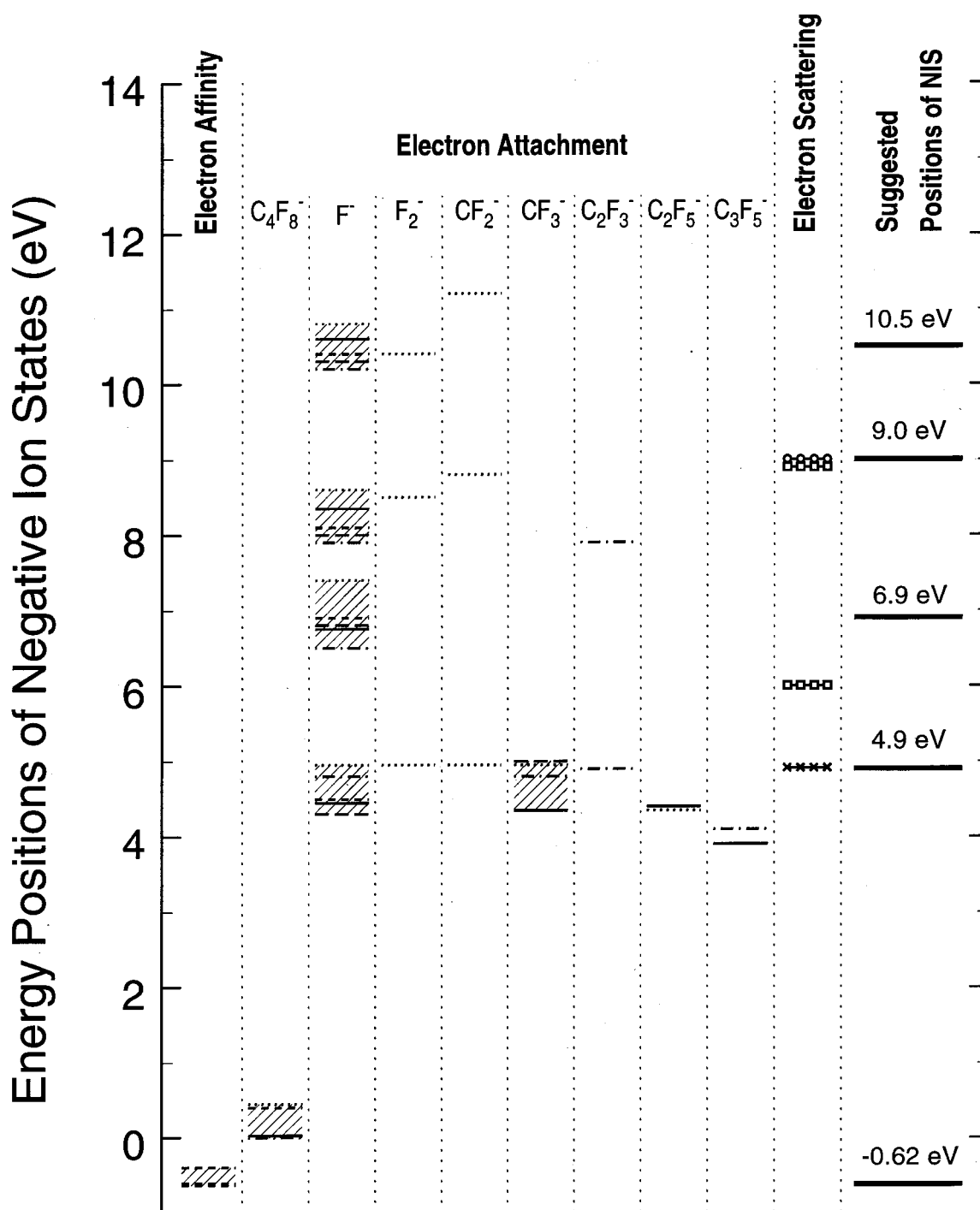
FIG. 1. Energy positions, E_{NIS}, of the negative ion states of c-C_4F_8 below 12 eV as obtained from electron affinity, electron attachment, and electron scattering studies. Electron affinity values: see Table 2 and the text. Electron attachment values: $(\cdots)$, Ref. 54; (—), Ref. 47; $(- \cdot -)$ Ref. 51; $(- - -)$ Ref. 53; $(- -)$ Ref. 49. Electron scattering values: $(\times - \times)$ Ref. 56; $(\square - \square)$ Ref. 57; $(\bigcirc - \bigcirc)$ Refs. 58, 59. The peak at 1.75 eV observed in Ref. 47 for F^- and $C_3F_5^-$ is not shown in the figure since it has not been reproduced by any of the other studies.

about 20 and 40 eV. These energies are outside the energy region where cross-section enhancements due to negative ion states are normally expected.

The disparity between the two sets of cross section measurements makes it difficult to recommend cross section values for the $\sigma_{\text{sc,t}}(\varepsilon)$ of c-C_4F_8. However, we obtained suggested values for $\sigma_{\text{sc,t}}(\varepsilon)$ between 1.1 and 3000 eV by

determining the least squares average of the two sets of measurements in the overlapping energy range of 4–20 eV, and by extending the suggested values to higher and lower energies by normalizing the high energy ($\geqslant 20$ eV) cross section data of Nishimura to the average at 20 eV and the low energy ($\leqslant 4$ eV) cross section data of Sanabia *et al.* to the average at 4 eV. The resultant suggested cross section $\sigma_{\text{sc,t}}(\varepsilon)$ is shown
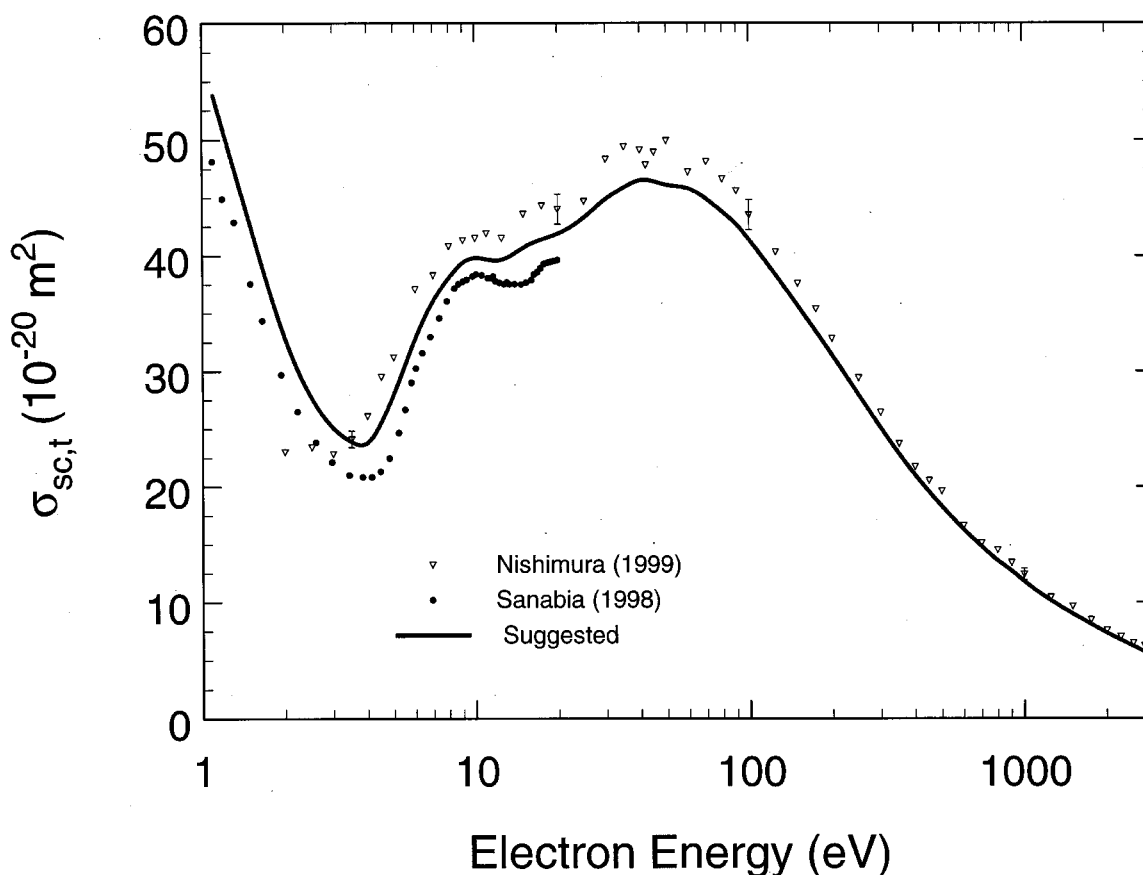
FIG. 2. Total electron scattering cross section, $\sigma_{sc,t}(\varepsilon)$, of c-C_4F_8: ($\bullet$) Ref. 57; ($\triangledown$) Refs. 58, 59; (—) suggested (see text).

in Fig. 2 by the solid line, and values obtained from this line are listed in Table 4.

3.2. Differential elastic electron scattering cross sections, $\sigma_{e,diff}$

Figure 3 shows the recent measurements of $\sigma_{e,diff}$ of c-C_4F_8 by Okamoto and co-workers[60,61] and the calculated values of $\sigma_{e,diff}$ by McKoy and co-workers.[62] The agreement between the calculated and the measured values of $\sigma_{e,diff}$ is improved as the electron energy is increased. The $\sigma_{e,diff}$ functions show pronounced variations with scattering angle at all electron energies (1.5–100 eV) employed in these investigations. The experimental data for $\sigma_{e,diff}$ are listed in Table 5.

Values of the integral elastic electron scattering cross section $\sigma_{e,int}(\varepsilon)$ and the momentum transfer cross section $\sigma_m(\varepsilon)$ may be calculated by extrapolating the $\sigma_{e,diff}$ data to $0°$ and $180°$ and integrating the curve over all angles. However, these extrapolations and calculations have not been performed in the literature.

3.3. Differential vibrational excitation cross section, $\sigma_{vib,diff}(\varepsilon)$

Figure 4 shows the recent measurements of Tanaka and co-workers[61] of the vibrational differential excitation cross

section for an energy loss $\Delta\varepsilon = 0.15$ eV and a scattering angle θ of $50°$. The major peak near 7.5 eV, the rise of the cross section below 3 eV, and the cross section enhancements at ~ 4.9 and ~ 11 eV are attributable to the existence of negative ion states at these energies in agreement with the electron attachment and other electron scattering data listed in Table 3. The data in Fig. 4 show the significance of indirect vibrational excitation of the c-C_4F_8 molecule by electron impact.

4. Electron Impact Ionization

4.1. Partial ionization cross sections, $\sigma_{i,partial}(\varepsilon)$

There have been two measurements of the partial ionization cross sections $\sigma_{i,partial}(\varepsilon)$ of c-C_4F_8, the first by Toyoda et al.[63] and the second by Jiao et al.[64,65] Toyoda et al.[63] used quadrupole mass spectrometry and measured the cross sections for dissociative ionization of the c-C_4F_8 molecule by electron impact leading to the formation of CF^+, CF_2^+, CF_3^+, $C_2F_3^+$, $C_2F_4^+$, and $C_3F_5^+$ from threshold to 117.8 eV. Their cross section measurements have an uncertainty of about $\pm 10\%$ and are presented in Table 6 and Fig. 5. Jiao et al.[64,65] measured the $\sigma_{i,partial}(\varepsilon)$ of c-C_4F_8 from 16 to 200 eV using Fourier transform mass spectrometry. They detected 13 fragment positive ions (see Fig. 5 and Table 7) as opposed to the six reported by Toyoda et al. The absolute

TABLE 4. Suggested values for the total electron scattering cross section, $\sigma_{sc,t}(\varepsilon)$, of c-C_4F_8

Electron energy (eV)	$\sigma_{sc,t}(\varepsilon)$ $(10^{-20}\,m^2)$	Electron energy (eV)	$\sigma_{sc,t}(\varepsilon)$ $(10^{-20}\,m^2)$
1.1	53.8	40.0	46.5
1.5	42.6	45.0	46.4
2.0	32.9	50.0	46.1
2.5	27.7	60.0	45.8
3.0	25.1	70.0	44.9
3.5	23.9	80.0	43.8
4.0	23.8	90.0	42.7
4.5	25.6	100	41.4
5.0	28.0	150	35.7
6.0	32.8	200	31.4
7.0	36.1	300	25.1
8.0	38.1	400	21.0
9.0	39.4	500	18.3
10.0	39.8	600	16.3
12.0	39.6	700	14.8
13.0	39.8	800	13.6
15.0	40.7	900	12.7
17.0	41.3	1000	11.8
20.0	41.9	1500	9.00
25.0	43.3	2000	7.35
30.0	44.9	2500	6.20
35.0	45.9	3000	5.29

values of their partial ionization cross sections were obtained by normalization to those of Wetzel et al.[66] for argon and have an uncertainty of about $\pm 20\%$. They are listed in Table 7 and are compared in Fig. 5 with those of Toyoda et al. and with some early measurements for the production of CF_3^+, $C_2F_4^+$, and $C_3F_5^+$ at 35 eV by Bibby and Carter.[49]

There are substantial differences between the two sets of measurements which depend on the particular positive ion fragment involved. The parent positive ion c-$C_4F_8^+$ was not detected in either of these electron-impact studies[63,64] or in the photon-impact study of Jarvis et al.,[46] indicating that the ground state of the c-$C_4F_8^+$ ion is not bound in the Franck-Condon region. Nevertheless, Smith and Kevan[67] reported observation of a weak c-$C_4F_8^+$ signal in studies of the total and dissociative charge-transfer cross sections of Xe^+ with c-C_4F_8. These latter observations may indicate a minimum in the potential energy surface of c-$C_4F_8^+$ at large internuclear separation distances.

In Table 8 are listed the energy thresholds for the appearance of a number of positive ions by electron (and photon) impact on c-C_4F_8.

4.2. Total ionization cross section, $\sigma_{i,t}(\varepsilon)$

In Fig. 6 is plotted the sum of the partial ionization cross sections of Toyoda et al.[63] and, similarly, the sum of the partial ionization cross sections of Jiao et al.[65] (the ''structure'' in the data of Jiao et al. may not be real). In addition, Bibby and Carter[49] made an early measurement of the partial ionization cross section for the production of CF_3^+, $C_2F_4^+$, and $C_3F_5^+$ from c-C_4F_8 at only one value (35 eV) of the incident electron energy. The sum of the partial cross sections of these three positive-ion fragments is $5.35 \times 10^{-20}\,m^2$ and is shown in Fig. 6. Also shown in Fig. 6 are two earlier measurements of the total ionization cross section, one by Kurepa[53] and the other by Beran and Kevan.[68] The former measurements were made at incident electron energies ranging from threshold to 100 eV and the latter at an incident electron energy of 70 eV. The differences between the various measurements is probably within the combined uncertainty considering the fact that the values of Toyoda et al. do not include the contributions of some of the weaker ions measured by Jiao et al. (The sum of the cross sections, at 70 eV, of the seven fragment ions reported by Jiao et al. but not by Toyoda et al. is $1.1 \times 10^{-20}\,m^2$). A suggested cross section $\sigma_{i,t}(\varepsilon)$ has been derived by a fit to the two most recent measurements which are in reasonable agreement with the earlier measurements of Beran and Kevan[68] and Bibby and Carter.[49] The suggested cross section is shown in Fig. 6 by the solid line and values derived from this fit are listed in Table 9.

It should be noted that since CF_2 may be the most abundant radical in the electron-impact dissociation of the c-C_4F_8 molecule into neutral fragments, electron-impact ionization of this radical may also be important in c-C_4F_8 plasmas. The electron-impact ionization cross section of the CF_2 radical has been measured by Tarnovsky and Becker[69] (see also Ref. 22).

4.3. Density-reduced ionization coefficient, $\alpha/N(E/N)$

There have been two experimental determinations of the density-reduced ionization coefficient $\alpha/N(E/N)$ of this molecule by Naidu et al.,[70] over the E/N range from $\sim 300 \times 10^{-17}$ to $\sim 650 \times 10^{-17}\,V\,cm^2$, and by Tagashira et al.[71] for three values of E/N (394×10^{-17}, 425×10^{-17}, and $455 \times 10^{-17}\,V\,cm^2$). The measurements of Naidu et al. were conducted at a gas temperature of 293 K and at two values of the gas pressure, namely 0.084 and 0.1333 kPa. No pressure dependence was observed in their measurements of this quantity. According to Naidu et al., the uncertainty of their data is about $\pm 10\%$ at values of E/N below $(E/N)_{lim}$ and about $\pm 20\%$ at higher E/N values $[(E/N)_{lim}$ is the value of (E/N) for which $\alpha = \eta$, where η is the attachment coefficient (Sec. 6)]. These data are plotted in Fig. 7. The solid line is a least squares fit to the data, and values obtained from the fit are listed in Table 10. These values should be treated with caution until they are validated by additional measurements. If these data are used in conjunction with the density-reduced electron attachment coefficient, $\eta/N(E/N)$, of Naidu et al.[70] to determine the density-reduced effective ionization coeffi-

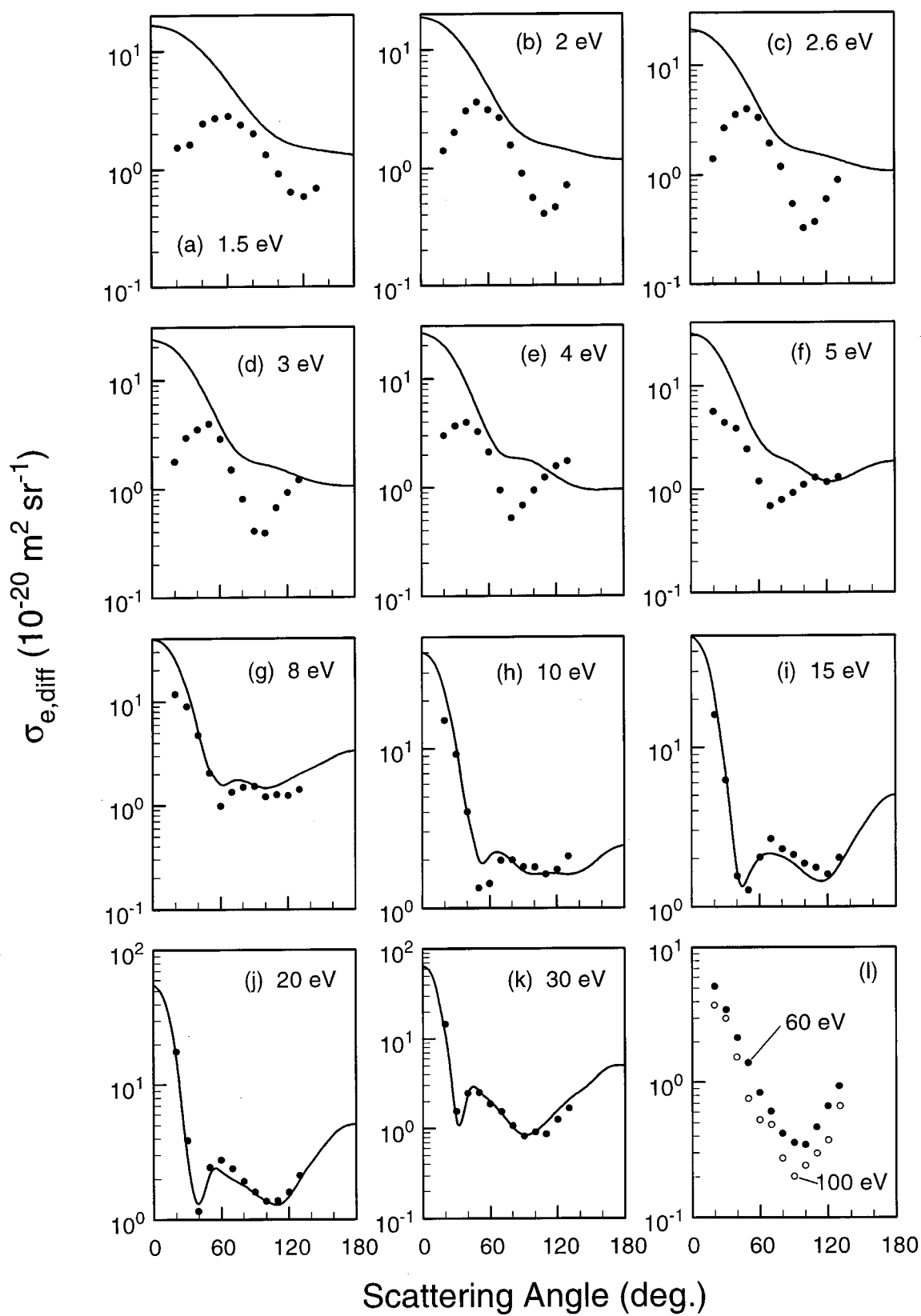FIG. 3. Differential elastic electron scattering cross sections, $\sigma_{e,diff}$, for c-C₄F₈: ($\bullet$,$\circ$) data of Tanaka and co-workers[60, 61]; (—) calculations of McKoy et al.[62]

TABLE 5. Differential elastic electron scattering cross sections,[a] $\sigma_{e,diff}$, for c-C_4F_8 in units of $10^{-20}\,m^2\,sr^{-1}$

	Electron energy (eV)												
Angle	1.5	2	2.6	3	4	5	8	10	15	20	30	60	100
20°	1.52	1.40	1.40	1.77	3.00	5.59	11.8	15.0	16.0	17.7	14.5	5.14	3.75
30°	1.62	1.99	2.66	2.95	3.66	4.37	8.98	9.20	6.22	3.85	1.54	3.46	2.99
40°	2.43	3.04	3.52	3.49	3.96	3.83	4.73	3.99	1.55	1.15	2.45	2.14	1.53
50°	2.68	3.59	3.97	3.93	3.25	2.42	2.04	1.33	1.27	2.44	2.50	1.39	0.755
60°	2.81	3.09	3.31	2.84	2.09	1.19	0.98	1.41	2.02	2.76	1.87	0.837	0.526
70°	2.38	2.65	1.94	1.49	0.941	0.683	1.33	1.97	2.65	2.38	1.53	0.608	0.484
80°	1.99	1.55	1.18	0.803	0.519	0.784	1.49	1.99	2.28	1.92	1.06	0.416	0.273
90°	1.33	0.897	0.543	0.407	0.683	0.913	1.52	1.79	2.10	1.59	0.813	0.358	0.201
100°	0.910	0.555	0.325	0.388	0.936	1.10	1.20	1.79	1.85	1.36	0.907	0.345	0.242
110°	0.633	0.406	0.370	0.666	1.23	1.29	1.25	1.62	1.74	1.37	0.862	0.464	0.298
120°	0.583	0.460	0.601	0.923	1.56	1.17	1.24	1.73	1.59	1.59	1.25	0.667	0.372
130°	0.683	0.707	0.898	1.20	1.74	1.30	1.41	2.10	2.01	2.11	1.67	0.933	0.667

[a]Data of Okamoto and co-workers,[60, 61] obtained by digitizing data appearing in figures.

cient, $(\alpha - \eta)/N\,(E/N)$, the resultant values differ from the two available direct measurements of $(\alpha - \eta)/N$ (see Fig. 8).

The limited measurements of Tagashira *et al.*[71] exhibited a pronounced decrease of α/N with increasing c-C_4F_8 gas pressure (from ~ 0.33 to ~ 5.3 kPa). No explanation was provided for this observation, which, if valid, would imply that the data of Naidu *et al.* are appropriate only for the gas pressures used in their measurements. The measurements of Tagashira *et al.* need to be repeated, expanded, and further scrutinized to confirm this reported pressure dependence.

4.4. Density-reduced effective ionization coefficient, $(\alpha - \eta)/N\,(E/N)$

There have been two direct measurements of the density-reduced effective ionization coefficient, $(\alpha - \eta)/N\,(E/N)$, of
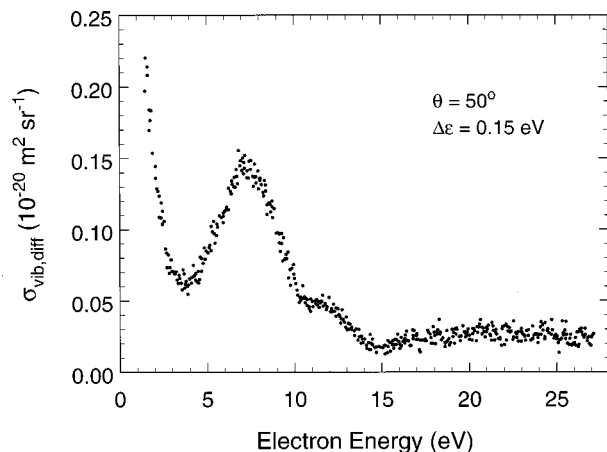
FIG. 4. Vibrational differential electron scattering cross section, $\sigma_{vib,diff}\,(\varepsilon)$, for c-C_4F_8 (data of Tanaka *et al.*[61]).

c-C_4F_8 using the pulsed Townsend method, one by Wen and Wetzer[72] and the other by de Urquijo.[73] These are compared in Fig. 8. The measurements by Wen and Wetzer[72] were conducted at a pressure of 0.1333 kPa and those by de Urquijo[73] at gas pressures ranging from 0.08 to 1 kPa. The latter data indicate that $(\alpha - \eta)/N\,(E/N)$ is pressure dependent in the pressure range covered by this study. The decrease in $(\alpha - \eta)/N\,(E/N)$ with N seems to be consistent with the decrease of α/N observed by Tagashira *et al.*[71] Although this pressure dependence may originate from "secondary" electron attachment processes (electron scattering via high-lying negative ion states and attachment of the slowed-down electrons by c-C_4F_8 via the near-zero electron attachment process forming c-$C_4F_8^-$) and from the effect of such indirect electron scattering on the electron energy distribution function, presently there are no quantitative measurements to support such an interpretation.

Also shown in Fig. 8 are $(\alpha - \eta)/N\,(E/N)$ values obtained using the data of Naidu *et al.*[70] for $\alpha/N\,(E/N)$ and $\eta/N\,(E/N)$ (see Fig. 17 in Sec. 6.8) which were measured using the steady-state Townsend method. These data differ from the direct measurements of $(\alpha - \eta)/N\,(E/N)$. The data of Naidu *et al.* give for the limiting E/N, $(E/N)_{lim}$, (E/N at which $\alpha/N = \eta/N$) a value of $359 \times 10^{-17}\,V\,cm^2$ which is much lower than the value of $434 \times 10^{-17}\,V\,cm^2$ determined by Wen and Wetzer[72] and those inferred from the de Urquijo measurements (see Fig. 8). It is also much lower than the room-temperature values of the uniform-field breakdown strength $(E/N)_{Br}$ measured by Berril *et al.*[74] and Christophorou *et al.*[75] for this gas. The Berril *et al.* measurements of $(E/N)_{Br}$ ranged from 428×10^{-17} to $432 \times 10^{-17}\,V\,cm^2$ and were made at pressures between 10.1 and 60.6 kPa. The value of $(E/N)_{Br}$ measured by Christophorou *et al.*[75] is 438 $\times 10^{-17}\,V\,cm^2$ and was made at 69.3 kPa. These compari-

TABLE 6. Partial ionization cross sections,[a] $\sigma_{i,partial}(\varepsilon)$, for c-C_4F_8

Electron energy (eV)	$\sigma_{i,partial}(\varepsilon)$ (10^{-20} m^2)						
	CF^+	CF_2^+	CF_3^+	$C_2F_3^+$	$C_2F_4^+$	$C_3F_5^+$	Sum
12.8					0.0072	0.0032	0.010
14.8			0.0004				
15.3			0.0007		0.0871	0.0254	0.113
17.8	0.0043	0.0001	0.0115		0.297	0.093	0.406
20.3	0.0342	0.0032	0.0819	0.0001	0.608	0.250	0.977
22.8	0.102	0.0189	0.265	0.0013	0.917	0.439	1.74
25.3	0.215	0.0516	0.573	0.0060	1.17	0.621	2.64
27.8	0.532	0.0984	0.903	0.0137	1.42	0.814	3.78
30.3	0.765	0.146	1.19	0.0262	1.66	1.00	4.79
32.8	1.09	0.195	1.44	0.0362	1.93	1.17	5.86
35.5	1.33	0.245	1.63	0.0440	2.12	1.31	6.68
37.3	1.67	0.303	1.78	0.0513	2.32	1.46	7.58
40.3	1.93	0.341	1.92	0.0557			8.25
42.8	2.21	0.382	2.06	0.0590	2.54	1.69	8.94
45.3	2.42	0.413		0.0631			9.41
47.8	2.67	0.444	2.16	0.0668	2.72	1.85	9.91
50.3	2.81	0.470					10.3
52.8	2.99	0.490	2.28	0.0690	2.93	1.93	10.7
57.8	3.14	0.515	2.30	0.0711	3.00	2.07	11.1
62.8	3.24	0.545	2.35	0.0715	3.11	2.16	11.5
67.8	3.32	0.551	2.39	0.0712	3.15	2.23	11.7
72.8	3.33	0.555	2.45	0.0705	3.12	2.25	11.8
77.8	3.36	0.571	2.47	0.0705	3.17	2.29	11.9
82.8	3.40	0.573	2.48	0.0695	3.18	2.32	12.0
87.8	3.43	0.573	2.48	0.0691	3.17	2.36	12.1
92.8	3.42	0.577	2.48	0.0684	3.16	2.38	12.1
97.8	3.44	0.580	2.46	0.0682	3.17	2.41	12.1
107.8	3.49	0.582	2.43	0.0673	3.16	2.43	12.2
117.8	3.52	0.579	2.41	0.0672	3.21	2.46	12.2

[a]Data of Toyoda et al.[63]

sons would indicate that the measurements of Naidu et al.[70] for both $\alpha/N(E/N)$ and $\eta/N(E/N)$ require validation by independent measurements.

5. Dissociation into Neutral Fragments

Toyoda et al.[63] used appearance mass spectrometry in a dual electron beam system to measure the absolute cross sections, $\sigma_{dis,partial}(\varepsilon)$, for electron-impact dissociation of c-C_4F_8 into the neutral radicals CF, CF$_2$, and CF$_3$ from threshold to 250 eV. These cross sections, along with their sum, are shown in Fig. 9 and are listed in Table 11. The sum of these partial dissociation cross sections must be taken as a lower limit of the total cross section $\sigma_{dis,neu,t}(\varepsilon)$ for dissociation of c-C_4F_8 into neutrals by electron impact, because other neutral fragments for which the cross sections have not

been measured will contribute to $\sigma_{dis,neu,t}(\varepsilon)$. For instance, Toyoda et al.[63] observed C$_3$F$_5$ radicals, but reported only the relative cross section for their formation. The stated absolute and relative uncertainties of the cross sections $\sigma_{dis,partial}(\varepsilon)$ are, respectively, $\pm 100\%$ and $\pm 20\%$.[63] However, similar cross sections obtained by the same group for other molecules, such as CF$_4$ and CHF$_3$, have been shown to be significantly smaller than their true values.[28] The threshold energies for the production of the neutral fragments CF, CF$_2$, and CF$_3$ by electron impact on c-C_4F_8 as determined by Toyoda et al. are, respectively, 14.5, 10.5, and 12.8 eV.

A model calculation predicting radical composition in c-C_4F_8 plasmas was conducted by Kazumi et al.[76] This calculation predicts the production of a number of other radicals besides those detected in the measurements of Toyoda et al.[63]

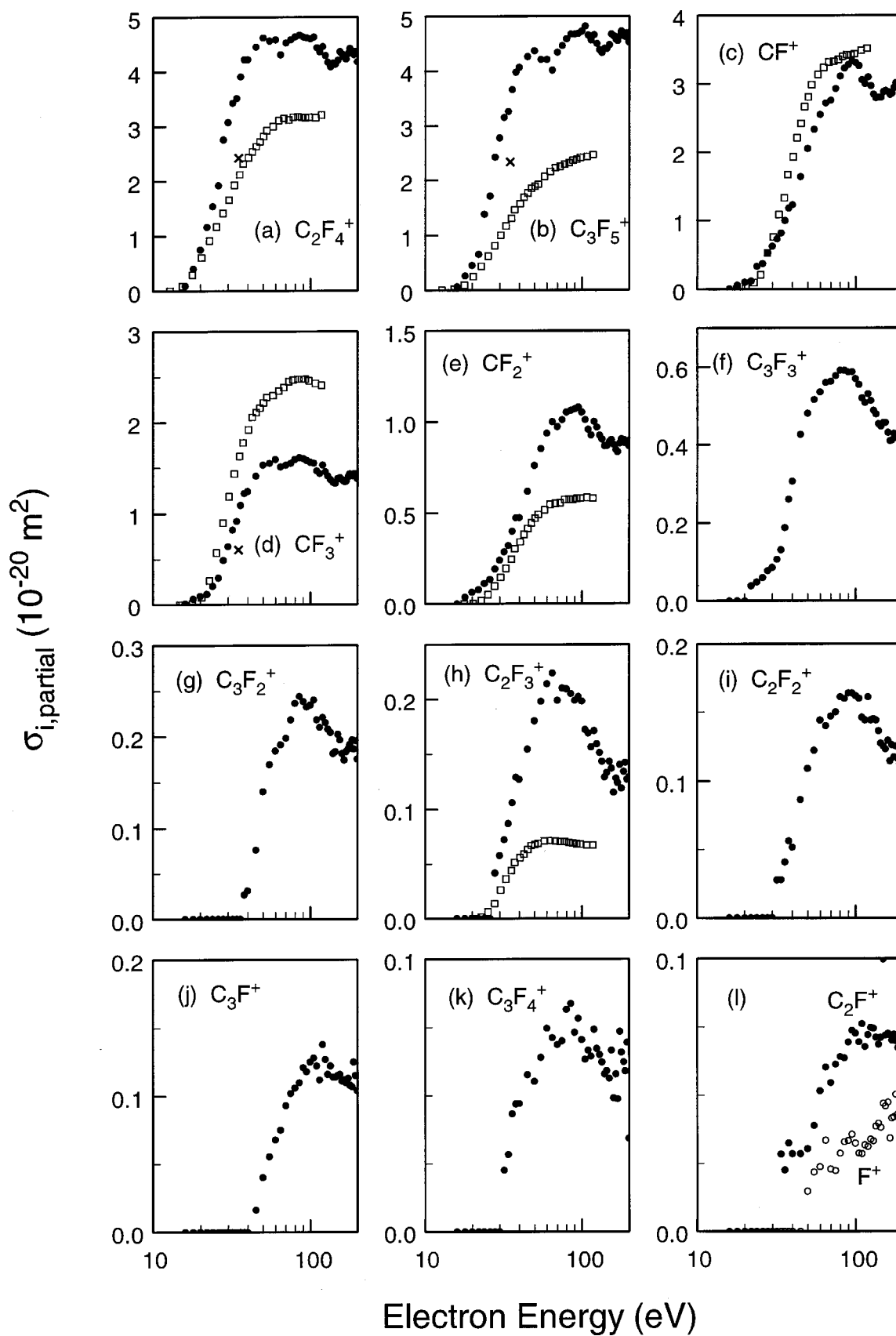FIG. 5. Partial ionization cross sections, $\sigma_{i,\text{partial}}(\varepsilon)$, of c-C_4F_8: ($\square$) data of Toyoda *et al.*[63]; ($\bullet$,$\bigcirc$) data of Jiao *et al.*;[65] ($\times$) data of Bibby and Carter.[49]

TABLE 7. Partial ionization cross sections, $\sigma_{\text{i,partial}}(\varepsilon)$, for c-C$_4F_8$[a]

Electron energy (eV)	$\sigma_{\text{i,partial}}(\varepsilon)$ (10^{-20} m^2)													
	F$^+$	CF$^+$	C$_2$F$^+$	CF$_2^+$	C$_3$F$^+$	C$_2$F$_2^+$	CF$_3^+$	C$_3$F$_2^+$	C$_2$F$_3^+$	C$_3$F$_3^+$	C$_2$F$_4^+$	C$_3$F$_4^+$	C$_3$F$_5^+$	Sum
16		0.008					0.010				0.087		0.065	0.170
18		0.056		0.036			0.063				0.405		0.263	0.823
20		0.103		0.064			0.090				0.749		0.449	1.46
22		0.117		0.076			0.115			0.038	1.16		0.655	2.16
24		0.334		0.112			0.202			0.048	1.54		1.38	3.62
26		0.374		0.135			0.292			0.059	1.92		1.71	4.48
28		0.531		0.190			0.487		0.041	0.077	2.75		2.42	6.49
30		0.625		0.240			0.641		0.058	0.085	3.07		2.77	7.49
32		0.736		0.285		0.028	0.824		0.072	0.106	3.43	0.023	3.15	8.65
34		0.817	0.028	0.321		0.028	0.918		0.087	0.130	3.51	0.028	3.26	9.14
36		0.997	0.023	0.398		0.041	1.09		0.106	0.187	3.91	0.043	3.66	10.5
38		1.18	0.033	0.473		0.056	1.22	0.027	0.129	0.260	4.22	0.047	3.97	11.6
40		1.23	0.029	0.473		0.052	1.24	0.031	0.127	0.305	4.22	0.047	4.06	11.8
45		1.64	0.029	0.616	0.016	0.086	1.41	0.076	0.154	0.425	4.45	0.058	4.26	13.2
50	0.015	2.05	0.030	0.758	0.040	0.109	1.53	0.140	0.180	0.480	4.62	0.055	4.36	14.4
55	0.022	2.33	0.039	0.850	0.055	0.122	1.55	0.169	0.198	0.516	4.56	0.064	4.21	14.7
60	0.024	2.55	0.052	0.936	0.068	0.144	1.59	0.184	0.214	0.535	4.59	0.075	4.21	15.2
65	0.034	2.72	0.060	0.998	0.075	0.140	1.51	0.191	0.224	0.560	4.31	0.071	4.01	14.9
70	0.023	2.76	0.055	0.970	0.093	0.147	1.53	0.198	0.199	0.563	4.53	0.069	4.34	15.5
75	0.022	2.93	0.061	1.01	0.102	0.150	1.55	0.218	0.210	0.578	4.59	0.070	4.46	15.9
80	0.029	3.11	0.064	1.05	0.106	0.161	1.59	0.236	0.209	0.591	4.64	0.082	4.58	16.4
85	0.033	3.23	0.064	1.06	0.110	0.160	1.61	0.244	0.205	0.591	4.67	0.084	4.67	16.7
90	0.033	3.28	0.069	1.07	0.121	0.164	1.60	0.238	0.199	0.587	4.64	0.073	4.67	16.7
95	0.036	3.33	0.074	1.08	0.118	0.164	1.58	0.232	0.202	0.588	4.62	0.078	4.68	16.8
100	0.032	3.31	0.073	1.05	0.125	0.162	1.56	0.234	0.198	0.569	4.60	0.071	4.72	16.7
105	0.029	3.26	0.070	1.01	0.128	0.160	1.55	0.240	0.172	0.554	4.63	0.063	4.82	16.7
110	0.029	3.06	0.076	0.955	0.122	0.146	1.47	0.218	0.169	0.519	4.44	0.067	4.65	15.9
115	0.032	3.00	0.068	0.924	0.112	0.144	1.44	0.210	0.156	0.508	4.36	0.064	4.56	15.6
120	0.031	3.10	0.072	1.00	0.138	0.161	1.53	0.221	0.171	0.531	4.46	0.074	4.66	16.2
125	0.034	2.97	0.075	0.969	0.127	0.144	1.46	0.215	0.159	0.513	4.29	0.067	4.50	15.5
130	0.033	2.85	0.075	0.922	0.116	0.145	1.41	0.208	0.151	0.488	4.17	0.065	4.38	15.0
135	0.039	2.79	0.071	0.900	0.122	0.144	1.37	0.204	0.143	0.478	4.09	0.062	4.33	14.7
140	0.040	2.80	0.069	0.865	0.114	0.136	1.34	0.181	0.129	0.452	4.16	0.058	4.41	14.8
145	0.038	2.80	0.071	0.864	0.114	0.127	1.33	0.183	0.133	0.446	4.13	0.059	4.40	14.7
150	0.047	2.88	0.100	0.889	0.115	0.125	1.38	0.202	0.143	0.456	4.21	0.056	4.47	15.1
155	0.046	2.90	0.072	0.898	0.116	0.123	1.39	0.196	0.137	0.456	4.36	0.067	4.67	15.4
160	0.047	2.88	0.073	0.872	0.111	0.129	1.37	0.181	0.115	0.430	4.32	0.049	4.64	15.2
165	0.034	2.84	0.072	0.843	0.112	0.114	1.35	0.174	0.128	0.409	4.27	0.058	4.57	15.0
170	0.042	2.86	0.070	0.832	0.110	0.126	1.35	0.183	0.124	0.411	4.23	0.049	4.55	14.9
175	0.042	2.94	0.072	0.880	0.113	0.117	1.40	0.186	0.140	0.427	4.33	0.074	4.64	15.4
180	0.050	3.01	0.070	0.900	0.108	0.125	1.43	0.191	0.119	0.417	4.42	0.066	4.72	15.6
185	0.043	3.01	0.067	0.899	0.107	0.116	1.41	0.196	0.134	0.423	4.37	0.062	4.65	15.5
190	0.050	3.03	0.077	0.881	0.125	0.112	1.43	0.186	0.142	0.424	4.31	0.059	4.62	15.4
195	0.055	3.06	0.073	0.895	0.115	0.132	1.43	0.195	0.127	0.428	4.36	0.070	4.69	15.6
200	0.050	2.97	0.075	0.865	0.104	0.125	1.38	0.175	0.129	0.407	4.18	0.034	4.52	15.0

[a]Data of Jiao *et al.*[65]

6. Electron Attachment

6.1. Electron beam determined total electron attachment cross section $\sigma_{\text{a,t}}(\varepsilon)$

A number of electron beam studies[47,51–54] have shown that at electron energies below ~ 1 eV, the parent negative ion c-C$_4$F$_8^-$ is produced. The c-C$_4$F$_8^-$* initially formed by electron capture is unstable with respect to autodetachment.[77] Under single-collision conditions (low gas pressure) the lifetime of the isolated c-C$_4$F$_8^-$* ion toward autodetachment was found to be between 10 and 15 μs when measured using time-of-flight mass spectrometry,[51,54,78] and longer than ~ 200 μs when measured using ion-cyclotron resonance (ICR) techniques[79,80] (see Table 12). In the latter case the electrons normally have lower energies than in the former and this may explain the longer lifetime of c-C$_4$F$_8^-$* in the ICR measurements. For a number of other long-lived metastable molecular negative ions it has been found that their autodetachment lifetime decreases as the energy of the attached electron increases (e.g., see Refs. 77 and 81).

Kurepa[53] reported a total electron attachment cross section, $\sigma_{\text{a,t}}(\varepsilon)$, for c-C$_4F_8$ which below ~ 1 eV should represent the cross section for the formation of the parent negative ion c-C$_4$F$_8^-$ (see discussion later in this section). This cross

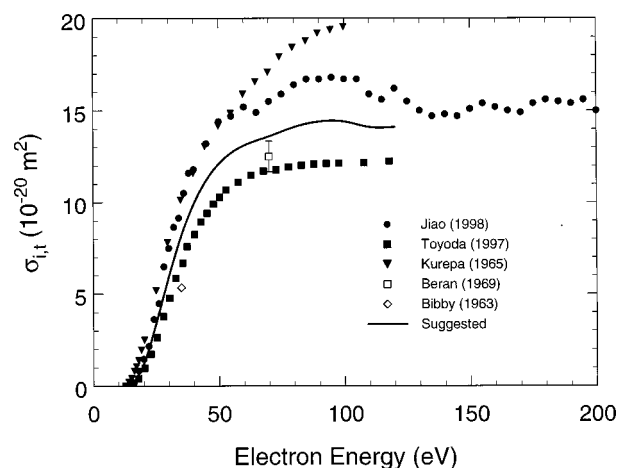TABLE 8. Energy thresholds for the appearance of positive-ion fragments by electron impact on c-C_4F_8

Positive ion fragment	Energy threshold (eV)	Reference
$C_3F_5^+$	11.6 ± 0.2^a	46
	12.1 ± 0.1	47
$C_2F_4^+$	11.8^a	46
	12.35 ± 0.1	47
CF_3^+	14.4 ± 0.2	47
	18.1	63
CF_2^+	20.3	63
CF^+	18.4 ± 0.2	47
	19.2	63

^{a}Photon-impact value, the rest of the data listed are electron-impact results.

TABLE 9. Suggested values for the total ionization cross section, $\sigma_{i,t}(\varepsilon)$, of c-C_4F_8

| Electron energy (eV)	$\sigma_{i,t}(\varepsilon)$ $(10^{-20}\,m^2)$	Electron energy (eV)	$\sigma_{i,t}(\varepsilon)$ $(10^{-20}\,m^2)$
14.0	0.02	40.0	9.92
15.0	0.07	45.0	11.2
16.0	0.21	50.0	12.1
17.0	0.42	60.0	13.1
18.0	0.66	70.0	13.6
19.0	0.89	80.0	14.1
20.0	1.21	90.0	14.4
25.0	3.44	100	14.4
30.0	5.93	110	14.1
35.0	8.18	120	14.1

TABLE 10. Values of the density-reduced ionization coefficient, $\alpha/N\,(E/N)$, for c-C_4F_8 derived from a fit to the data of Naidu et al.[70]

E/N $(10^{-17}\,V\,cm^2)$	$\alpha/N\,(E/N)$ $(10^{-18}\,cm^2)$
300	1.6
350	8.27
400	16.7
450	26.1
500	35.5
550	45.5
600	56.2
650	66.6

FIG. 6. Total ionization cross section, $\sigma_{i,t}(\varepsilon)$, of c-C_4F_8: ($\bullet$) Ref. 65; ($\blacksquare$) Ref. 63; ($\blacktriangledown$) Ref. 53; ($\square$) Ref. 68; ($\diamond$) Ref. 49; (—) suggested.

section is shown in Fig. 10. In plotting these data we assigned the maximum value of the cross section for the formation of c-$C_4F_8^-$ at 0.4 eV to be the value of 0.21 $\times 10^{-20}\,m^2$ listed by Kurepa in Table 5 of his paper.[53] In Fig. 10 is also plotted the low energy, electron-beam-determined cross section for the formation of c-$C_4F_8^-$ by Chutjian and Alajajian.[82] These investigators used their krypton photoionization technique and put their relative measurements on an absolute scale by normalization to the swarm data of Christodoulides et al.[83] These cross sections are discussed further in Sec. 6.5 where they are compared with the total electron attachment cross sections obtained from electron swarm data.

Prior to presenting and discussing the electron swarm data, we present and discuss here the relative cross section data obtained by electron beam investigations of the production of the various fragment negative ions formed by electron impact on c-C_4F_8. These studies[47,49,51,53–55,84] have shown the formation of many fragment negative ions via a number of negative ion states in the electron energy range between ~ 2 and ~ 15 eV. The most systematic measurements of the relative cross sections for the production of the various frag-
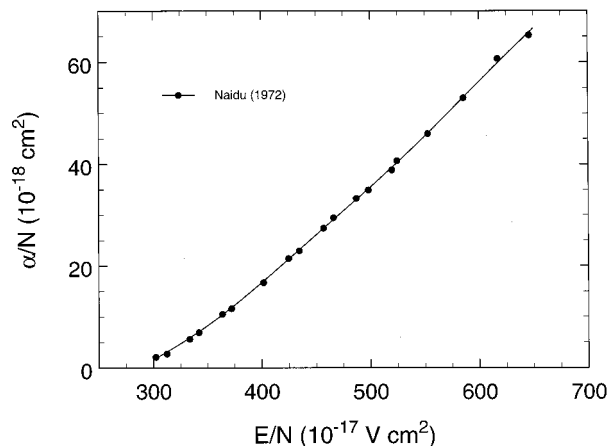
FIG. 7. Density-reduced ionization coefficient, $\alpha/N\,(E/N)$, for c-C_4F_8 (data of Naidu et al.[70]).
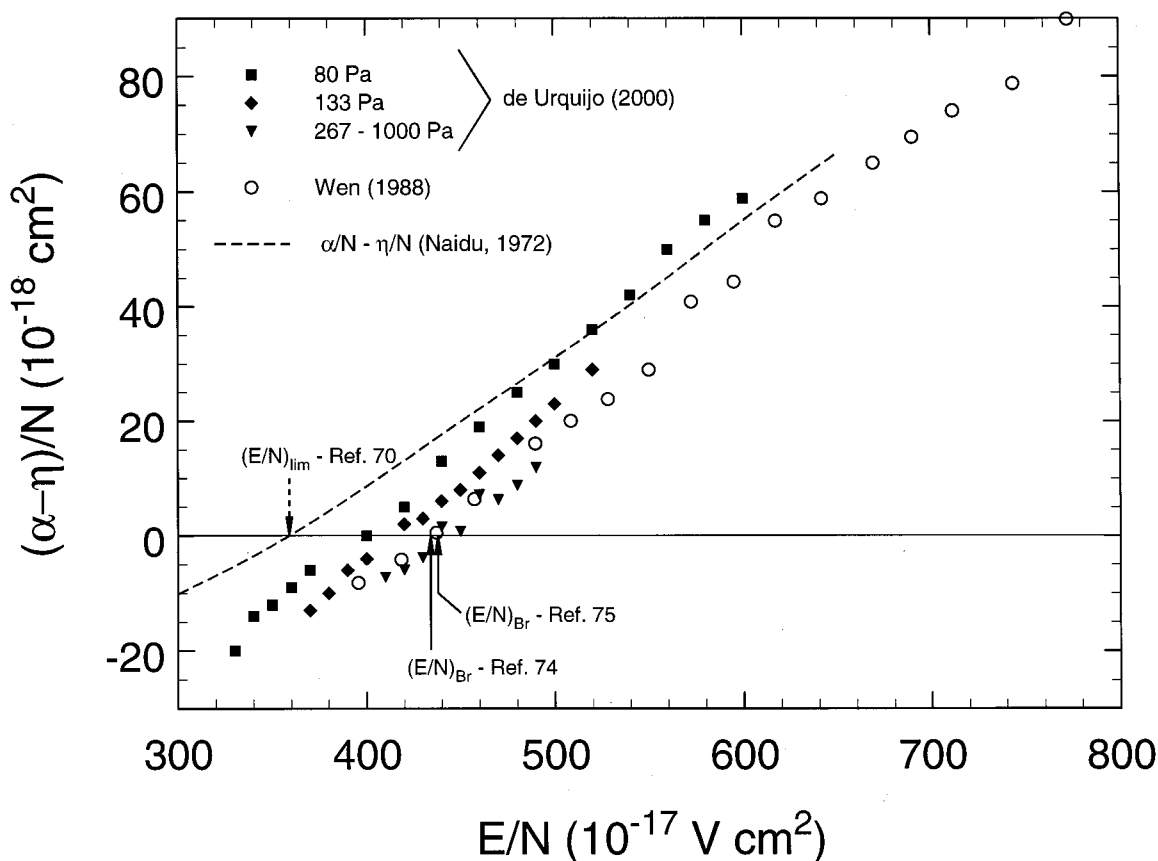
FIG. 8. Density-reduced effective ionization coefficient, $(\alpha - \eta)/N$ (E/N), for c-C$_4$F$_8$. (○) Ref. 72; (■,♦,▼) Ref. 73; (- - -, $\alpha/N - \eta/N$) Ref. 70; the broken arrow shows the $(E/N)_{\text{lim}}$ value of Ref. 70 and the solid arrows represent the values of $(E/N)_{\text{Br}}$ as measured in Refs. 72, 74 and 75.

ment negative ions as a function of the electron energy in absolute relation to each other were made by Sauers et $al.$[51] using time-of-flight mass spectrometry. These relative cross sections are shown in Fig. 11 along with the relative cross section for the production of the parent negative ion
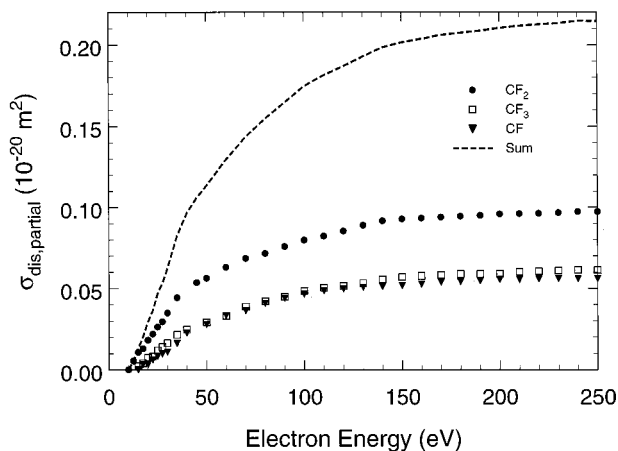

FIG. 9. Partial cross sections, $\sigma_{\text{dis,partial}}$ (ε), for electron-impact dissociation of c-C$_4$F$_8$ into the neutral fragments CF (▼), CF$_2$ (●), and CF$_3$ (□). The data are from Toyoda et $al.$,[63] and the broken line (- - -) represents the sum of the partial cross sections for the three fragments.

c-C$_4$F$_8^{-*}$ at electron energies below 1.5 eV. The most abundant fragment negative ion is seen to be F$^-$. This ion is formed via a number of negative ion states. Recent measurements[85] of the negative-ion density in a high density c-C$_4$F$_8$ plasma using a laser photodetachment technique, indicating the major negative ion species to be F$^-$, are consistent with these findings.

The other observed negative ion fragments (CF$_3^-$, C$_2$F$_3^-$, C$_3$F$_5^-$) have much lower cross sections than F$^-$ as they require multiple bond breaking and molecular rearrangement. All four fragment negative ions (F$^-$, CF$_3^-$, C$_2$F$_3^-$, and C$_3$F$_5^-$) are produced at electron energies between 4 and 5 eV, indicating the existence of a common negative ion state in this energy range. There is general agreement among the electron-beam studies[47,49,51,53–55,84] as to the positions of the various peaks in the relative yields of the various negative ions (see Table 3) except for the peak at 1.75 eV reported by Lifshitz and Grajower,[47] which was not observed in any of the other electron-beam studies.

Three of the electron-beam studies[49,53,55] reported absolute cross sections for some ions at their peak energies. These are summarized in Table 13. They disagree considerably with each other, and with the electron swarm data discussed later (Secs. 6.4 and 6.5) in this paper.

TABLE 11. Cross sections, $\sigma_{\text{dis,partial}}(\varepsilon)$, for electron-impact dissociation of c-C_4F_8 into the neutral fragments CF, CF_2, and CF_3.[a] The last column gives the sum of the cross sections in the preceding three columns

Electron energy (eV)	$\sigma_{\text{dis,partial}}(\varepsilon)$ $(10^{-20}\ \text{m}^2)$			
	CF	CF_2	CF_3	Sum
10		0.0002		0.0002
12.5		0.0055		0.0055
15	0.00016	0.0108	0.00244	0.0134
17.5	0.00335	0.0131	0.00419	0.0206
20	0.00345	0.0183	0.00771	0.0295
22.5	0.00618	0.0221	0.00824	0.0365
25	0.00850	0.0264	0.0120	0.0469
27.5	0.00976	0.0295	0.0141	0.0534
30	0.0110	0.0349	0.0165	0.0624
35	0.0163	0.0444	0.0216	0.0823
40	0.0227		0.0247	0.0964
45		0.0536		0.106
50	0.0279	0.0563	0.0292	0.113
60	0.0332	0.0630	0.0332	0.129
70	0.0362	0.0685	0.0388	0.144
80	0.0409	0.0716	0.0422	0.155
90	0.0439	0.0759	0.0448	0.165
100	0.0464	0.0798	0.0485	0.175
110	0.0486	0.0823	0.0505	0.181
120	0.0498	0.0854	0.0516	0.187
130	0.0506	0.0890	0.0533	0.193
140	0.0511	0.0917	0.0556	0.198
150	0.0517	0.0928	0.0570	0.202
160	0.0526	0.0933	0.0577	0.204
170	0.0538	0.0939	0.0583	0.206
180	0.0541	0.0944	0.0588	0.207
190	0.0547	0.0950	0.0588	0.209
200	0.0554	0.0958	0.0591	0.210
210	0.0554	0.0961	0.0601	0.212
220	0.0557	0.0963	0.0605	0.213
230	0.0558	0.0967	0.0608	0.213
240	0.0559	0.0973	0.0614	0.215
250	0.0560	0.0973	0.0612	0.215

[a]Data of Toyoda $et\ al.$[63]

TABLE 12. Autodetachment lifetime of c-$C_4F_8^{-*}$

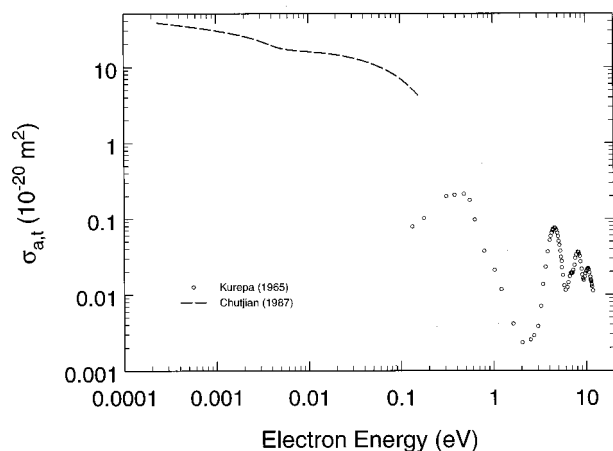| Lifetime (s)	Method of measurement	Reference
10×10^{-6}	Time-of-flight mass spectrometry	51
12×10^{-6}	Time-of-flight mass spectrometry	78
14.8×10^{-6}	Time-of-flight mass spectrometry	54
$\sim200\times10^{-6}$	Ion cyclotron resonance	79
500×10^{-6}	Ion cyclotron resonance	80

FIG. 10. Total electron attachment cross section, $\sigma_{a,t}(\varepsilon)$, as a function of electron energy for c-C_4F_8 measured using electron beam techniques: ($\bigcirc$) Ref. 53; ($--$) Ref. 82. The cross section below ~ 1 eV is due to the formation of c-$C_4F_8^-$.

6.2. Total electron attachment rate constant as a function of E/N, $k_{a,t}(E/N)$

There have been two measurements of the total electron attachment rate constant, $k_{a,t}(E/N)$, as a function of the density-reduced electric field E/N employing electron-swarm techniques and mixtures of c-C_4F_8 with the buffer gases of N_2 and Ar.[83,86] These room temperature ($T = 298$ K) measurements are shown in Fig. 12.

6.3. Total electron attachment rate constant as a function of the mean electron energy, $k_{a,t}(\langle \varepsilon \rangle)$

The total electron attachment rate constant, $k_{a,t}(\langle \varepsilon \rangle)$, as a function of the mean electron energy $\langle \varepsilon \rangle$ can be determined from the swarm measurements of $k_{a,t}(E/N)$ in the buffer gases N_2 and Ar shown in Fig. 12 since the electron energy
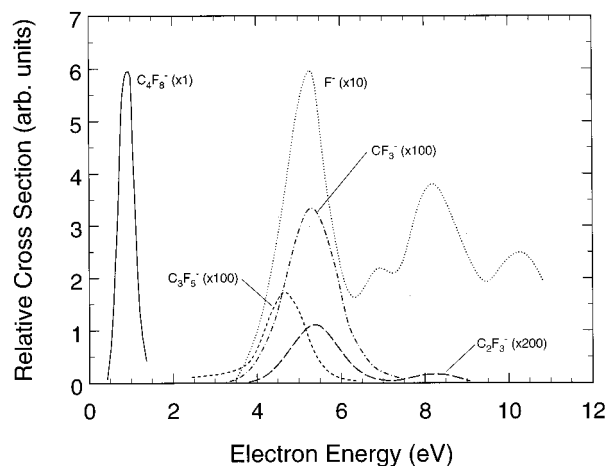
TABLE 13. Peak cross section values for negative ion fragments formed by electron impact on c-C_4F_8 (see text)

Peak cross section value (10^{-18} cm^2)	Peak energy (eV)	Fragment ion	Reference
236	4.3	F$^-$	49
0.9	4.95	F$^-$	55
7.56	4.5	total[a]	53
0.2	7.4	F$^-$	55
1.90	6.9	total[a]	53
0.4	8.6	F$^-$	55
3.60	8.1	total[a]	53
0.5	10.8	F$^-$	55
2.25	10.4	total[a]	53
11.1	5.0	CF$_3^-$	49
0.001	4.95	CF$_3^-$	55

[a]About equal to that for the production of F$^-$ at this energy.
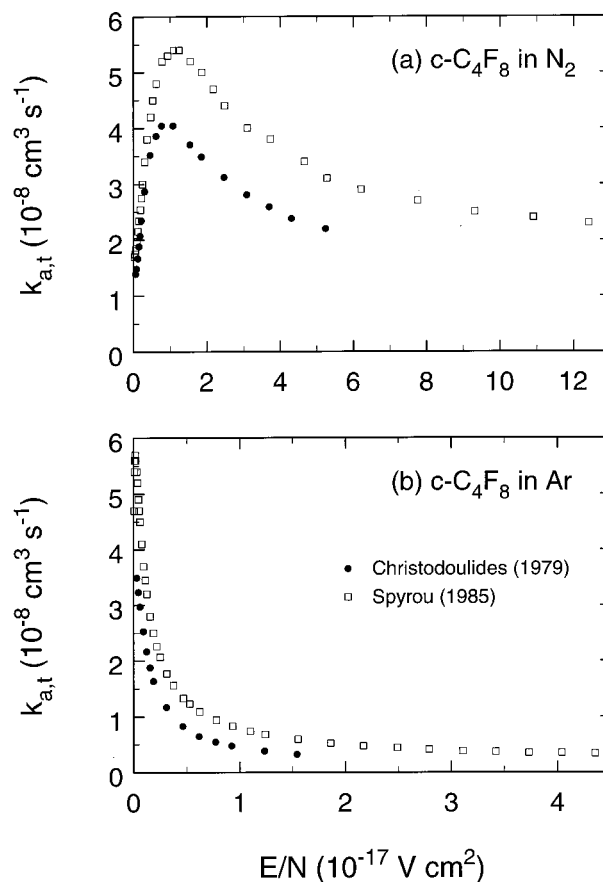
FIG. 12. Total electron attachment rate constant, $k_{a,t}(E/N)$, as a function of E/N for c-C_4F_8 measured in the buffer gas (a) N_2 and (b) Ar: ($\bullet$) Ref. 83; ($\square$) Ref. 86.

FIG. 11. Relative cross sections for the formation of the parent c-$C_4F_8^-$ and the fragment F$^-$, CF$_3^-$, C$_2$F$_3^-$, and C$_3$F$_5^-$ negative ions by electron attachment to c-C_4F_8 (note the multiplication factors) by Sauers et al.[51]

FIG. 13. Total electron attachment rate constant, $k_{a,t}(\langle\varepsilon\rangle)$, as a function of $\langle\varepsilon\rangle$ for c-C_4F_8: ($\bullet$) Ref. 87; ($\blacksquare$, $\square$) Ref. 83; ($\blacktriangledown$, $\triangledown$) Ref. 86; ($\blacklozenge$) Ref. 88; (—) recommended. Data shown by closed symbols were obtained in N_2 buffer gas, and data shown by open symbols were obtained in Ar buffer gas.

distribution function is known for each value of E/N at which the $k_{a,t}$ was measured in the buffer gases N_2 and Ar. These room-temperature ($T=298$ K) measurements of $k_{a,t}(\langle\varepsilon\rangle)$ are shown in Fig. 13, along with two other measurements of $k_{a,t}(\langle\varepsilon\rangle)$.[87,88] Although the differences between these four independent measurements of $k_{a,t}(\langle\varepsilon\rangle)$ from Christophorou's group are generally within the combined uncertainties (the individual uncertainties are about $\pm10\%$), the more recent values[86,88] are preferred. The solid line in Fig. 13 is a least squares fit to these data (taken in both N_2 and Ar buffer gases) and represents our recommended values for the $k_{a,t}(\langle\varepsilon\rangle)$ of c-C_4F_8. Values obtained from this line are listed in Table 14.
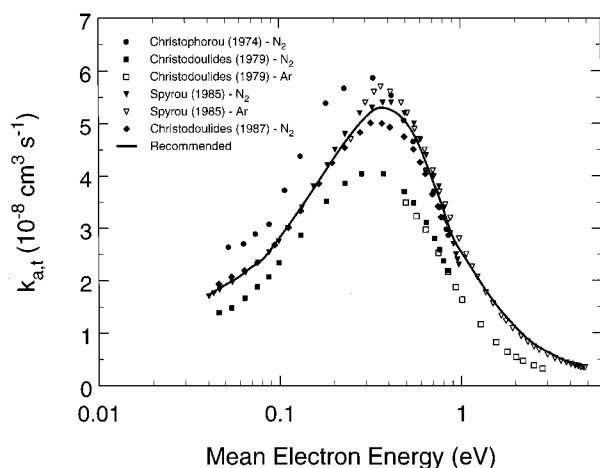
TABLE 14. Recommended values of the total electron attachment rate constant, $k_{a,t}(\langle\varepsilon\rangle)$, as a function of $\langle\varepsilon\rangle$ for c-C_4F_8

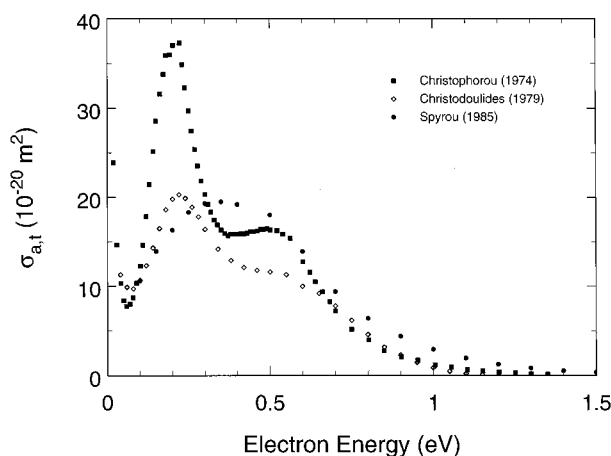| $\langle\varepsilon\rangle$ (eV)	$k_{a,t}(\langle\varepsilon\rangle)$ (10^{-8} cm^3 s^{-1})	$\langle\varepsilon\rangle$ (eV)	$k_{a,t}(\langle\varepsilon\rangle)$ (10^{-8} cm^3 s^{-1})
0.04	1.72	0.50	5.03
0.05	1.92	0.60	4.53
0.06	2.08	0.70	3.92
0.07	2.26	0.80	3.37
0.08	2.40	0.90	2.84
0.09	2.61	1.00	2.55
0.10	2.82	1.50	1.62
0.15	3.69	2.00	1.11
0.20	4.34	2.50	0.80
0.25	4.80	3.00	0.64
0.30	5.12	3.50	0.52
0.35	5.29	4.00	0.43
0.40	5.28	4.50	0.35

FIG. 14. Swarm-determined total electron attachment cross section, $\sigma_{a,t}(\varepsilon)$, as a function of electron energy ($\leqslant1.5$ eV) for c-C_4F_8: ($\blacksquare$) Ref. 87; ($\diamond$) Ref. 83; ($\bullet$) Ref. 86.

6.4. Swarm-unfolded total electron attachment cross section, $\sigma_{a,t}(\varepsilon)$

In Fig. 14 are shown the values of the total electron attachment cross section, $\sigma_{a,t}(\varepsilon)$, for c-C_4F_8 at energies below 1.5 eV. These have been obtained by Christophorou and co-workers[83,86,87] from an unfolding of their $k_{a,t}(E/N)$ data measured in mixtures of c-C_4F_8 with the buffer gases N_2[83,87] and Ar.[86] The respective electron energy distribution functions were used for each buffer gas. While the cross section from the most recent measurement exhibits a peak near 0.4 eV, the earlier data of Christophorou et al.[87] indicate a ''double peak'' with a distinct maximum near 0.2 eV. It may be possible that the peak near 0.2 eV in the earliest data resulted from unfolding errors or from an uncertainty in the electron energy distribution functions of N_2 that were used at the time. For this reason we shall not consider this cross section further.

6.5. Comparison of the values of $\sigma_{a,t}(\varepsilon)$ derived from electron swarm and electron beam experiments

In Fig. 15(a) are compared the values of $\sigma_{a,t}(\varepsilon)$ derived from electron swarm experiments[83,86,87] with the values of $\sigma_{a,t}(\varepsilon)$ derived from the electron-beam experiments of Kurepa[53] and Chutjian and Alajajian.[82] The data from the various sources differ considerably. Nonetheless, we have determined suggested values for the $\sigma_{a,t}(\varepsilon)$ of c-C_4F_8, which are shown by the solid line in Fig. 15(b), and are listed in Table 15.

These suggested values were obtained from a least-squares fit to the data in Fig. 15(b). These data are as follows: Below 0.06 eV the electron-beam data of Chutjian and Alajajian;[82] between 0.06 and 1.0 eV the electron swarm data of Christodoulides et al.[83] and Spyrou et al.;[86] between 1 and 3 eV the data of Spyrou et al.[86] derived from measurements in Ar buffer gas and normalized to the average of the Christodoulides et al.[83] and Spyrou et al.[86] data at 1 eV; and
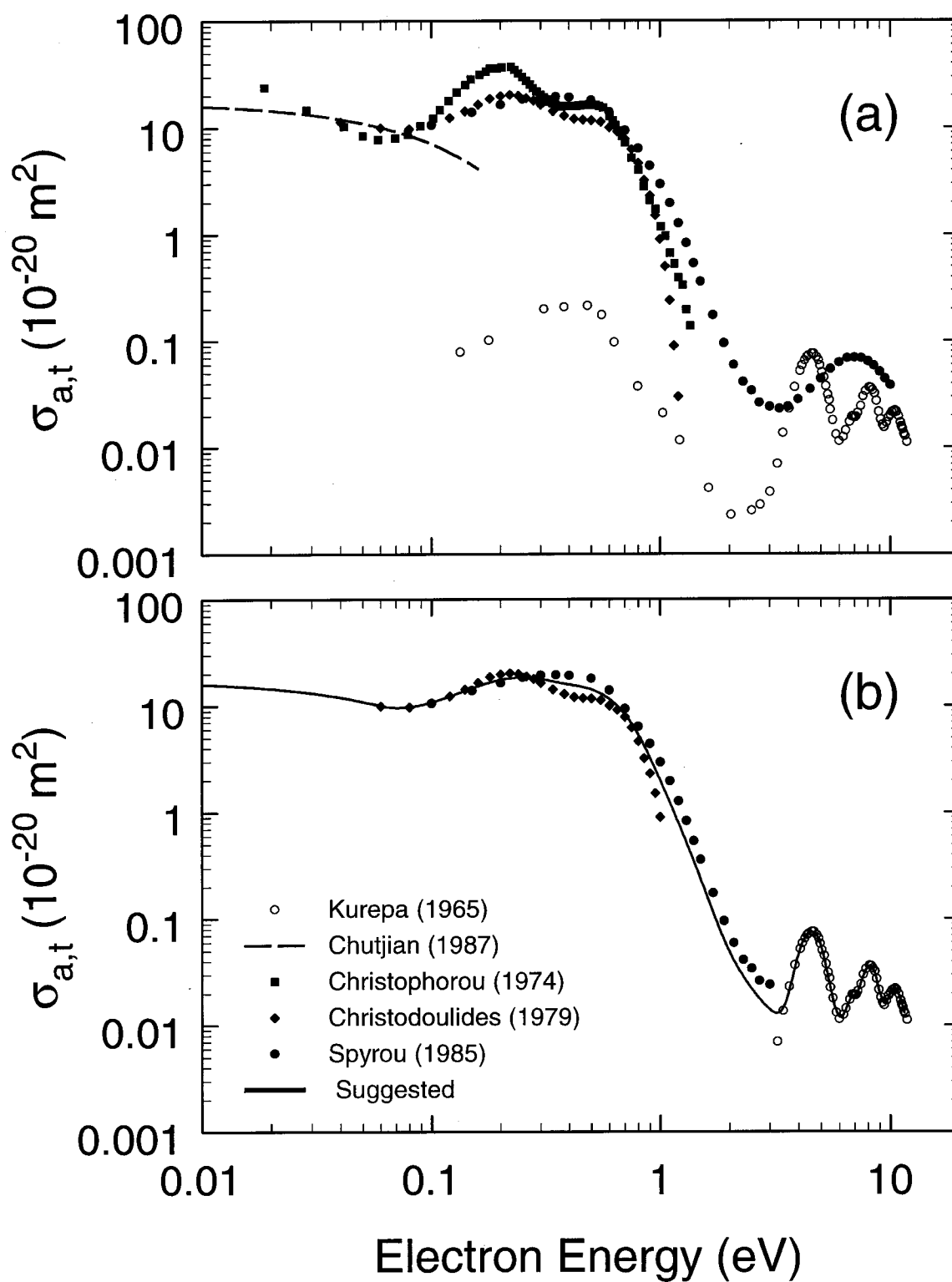
FIG. 15. (a) Comparison of electron swarm and electron beam data for the total electron attachment cross section, $\sigma_{a,t}(\varepsilon)$, of c-C_4F_8. Electron-swarm data: (■) Ref. 87; (♦) Ref. 83; (●) Ref. 86. Electron-beam data: (○) Ref. 53; (– –) Ref. 82. (b) Data of Ref. 82 (– –) below 0.06 eV (hidden behind solid line); data of Refs. 83 (♦) and 86 (●) between 0.06 and 3.0 eV; data of Ref. 53 (○) above 3 eV. (—) Suggested.

TABLE 15. Suggested values of the total electron attachment cross section, $\sigma_{a,t}(\varepsilon)$, of c-C_4F_8

Electron energy (eV)	$\sigma_{a,t}(\varepsilon)$ (10^{-20} m^2)	Electron energy (eV)	$\sigma_{a,t}(\varepsilon)$ (10^{-20} m^2)
0.010	15.9	1.5	0.235
0.015	15.2	2.0	0.049
0.02	14.5	2.5	0.022
0.03	13.2	3.0	0.014
0.04	12.0	3.5	0.016
0.05	10.9	4.0	0.047
0.06	10.0	4.5	0.075
0.07	9.67	5.0	0.055
0.08	9.83	5.5	0.022
0.09	10.2	6.0	0.012
0.10	10.8	6.5	0.015
0.15	14.6	6.75	0.018
0.20	17.5	7.0	0.019
0.25	18.4	7.25	0.021
0.30	17.8	7.5	0.026
0.35	16.7	8.0	0.035
0.40	15.8	8.5	0.032
0.45	15.1	9.0	0.020
0.5	14.2	9.5	0.016
0.6	11.5	10.0	0.020
0.7	8.22	10.5	0.022
0.8	5.35	11.0	0.018
0.9	3.24	11.5	0.013
1.0	1.97		

TABLE 16. Thermal values, $(k_{a,t})_{th}$, of the total electron attachment rate constant for c-C_4F_8

$(k_{a,t})_{th}$ (10^{-9} cm^3 s^{-1})	T (K)	Reference
0.4 ± 0.1^a	298	80
$8-9^{a,b}$	300	89, 90
11.1	300	91
12	298	83
12	298	92
13	298	16
15	300	21
16	298	86
16 ± 5	375	43
18.1	301	88
21	298	87

^{a}Measurements made using the ion cyclotron resonance technique. The rest of the data were obtained using electron swarm methods.
^{b}This value supersedes an earlier much higher value of 110×10^{-9} cm^3 s^{-1} published by the same group (Ref. 44) using the same method.

the electron swarm values because the electron attachment rate constant of c-C_4F_8 decreases as the electron energy approaches 0.0 eV (Fig. 13).

6.7. Total electron attachment rate constant as a function of the mean electron energy and gas temperature, $k_{a,t}(\langle\varepsilon\rangle,T)$

Christodoulides *et al.*[88] measured the total electron attachment rate constant as a function of E/N in N$_2$ buffer gas at a number of gas temperatures from 301 to 560 K. The $k_{a,t}(E/N,T)$ data were reported as $k_{a,t}(\langle\varepsilon\rangle,T))$ and are reproduced in Fig. 16. It is seen that the total electron attachment rate constant decreases with increasing gas temperature. Subsequent similar studies for other molecules which form parent negative ions and have electron affinities $\lesssim 0.5$ eV have shown that this ''negative'' temperature dependence is largely due to thermally induced electron detachment from the parent negative ion.[93]

6.8. Density-reduced electron attachment coefficient, $\eta/N(E/N)$

There has been only one experimental determination of the density-reduced electron attachment coefficient, $\eta/N(E/N)$, of c-C_4F_8 over an extended range of E/N, namely, that by Naidu *et al.*[70] shown in Fig. 17. These measurements were made at a temperature of 293 K and at two values of the gas pressure (0.084 and 0.133 kPa). They have a quoted uncertainty of about $\pm 10\%$ for E/N values below $(E/N)_{lim}$ and about $\pm 20\%$ for E/N values above $(E/N)_{lim}$. The solid line shown in Fig. 17 is a least squares fit to the data. Values obtained from this fit are listed in Table 17. For

above 3 eV the electron beam data of Kurepa.[53] The low energy data of Kurepa were not considered in view of the difficulty of the early electron beam methods in obtaining accurate cross sections for low electron energies. The swarm data of Christodoulides *et al.*[83] were not considered at energies in excess of 1 eV since these data were determined from measurements made only in mixtures with N$_2$. Similarly, the $\sigma_{a,t}(\varepsilon)$ data of Christophorou *et al.*[87] were not included for the reasons discussed in Sec. 6.4.

6.6. Thermal value, $(k_{a,t})_{th}$, of the total electron attachment rate constant

The published experimental data on $(k_{a,t})_{th}$ are listed in Table 16. If the lowest two measurements are excluded, the average of the remaining eight room-temperature measurements is 1.5×10^{-8} cm^3 s^{-1}. The lowest two values in Table 16 were measured using the ICR technique in which the electron energies are generally lower than the ''thermal'' electron energies in the electron swarm experiments. Thus the ICR-measured magnitudes of $(k_{a,t})_{th}$ may be lower than
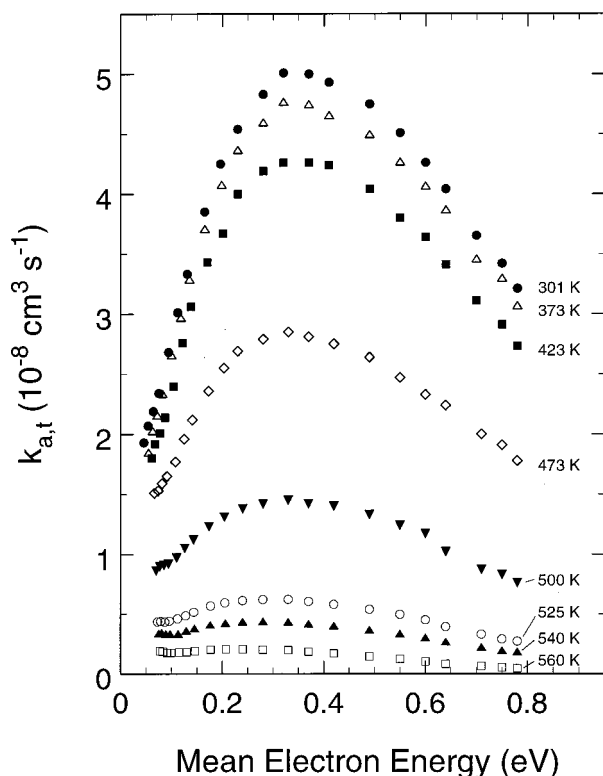
FIG. 16. Total electron attachment rate constant as a function of $\langle\varepsilon\rangle$ and T, $k_{a,t}(\langle\varepsilon\rangle,T)$, for c-C$_4F_8$ (data of Christodoulides et $al.$[88]).

TABLE 17. Values of η/N (E/N) for c-C$_4$F$_8$ ($T=293$ K) derived from a fit to the data of Naidu et $al.$[70]

E/N (10^{-17} V cm^2)	η/N (E/N) (10^{-18} cm^2)
300	11.8
350	9.98
400	8.10
450	6.22
500	4.49
550	2.87
600	1.25
625	0.43

293 K. The overall uncertainty in these data was quoted by Naidu et $al.$ to be less than $\pm5\%$. Also shown in Fig. 18 are the results of room temperature measurements of w (E/N) by Wen and Wetzer[72] and by de Urquijo.[73] The measurements by de Urquijo were obtained for a number of gas pressures (see figure legend), and seem to indicate a small decrease of the electron drift velocity with increasing gas pressure. The solid line shown in Fig. 18 is a least squares fit to the data of Naidu et $al.$, Wen and Wetzer, and de Urquijo. Values obtained from this line are listed in Table 18 as the presently suggested values for the w (E/N) of c-C$_4$F$_8$.

Measurements of w (E/N) in two mixtures of c-C$_4$F$_8$ with Ar at relative concentrations of 0.468% and 4.91% have recently been reported by Yamaji et $al.$[94] They may be of interest to those using Boltzmann codes for the calculation of electron transport parameters in c-C$_4$F$_8$.

the reasons discussed in Sec. 4.4, and the fact that limited measurements by Tagashira et $al.$[71] indicate a decrease in η/N with gas pressure, these values require further validation.

7. Electron Transport

7.1. Electron drift velocity, w (E/N)

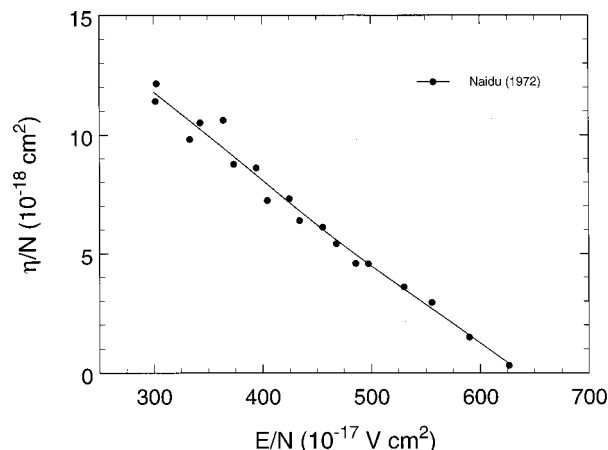In Fig. 18 are shown the measurements of Naidu et $al.$[70] for the electron drift velocity, w (E/N), in c-C$_4$F$_8$ made at

7.2. Ratio of the lateral electron diffusion coefficient to electron mobility, D_T/μ (E/N)

The D_T/μ (E/N) measurements by Naidu et $al.$[70] seem to be the only available data for this gas. They were obtained at 293 K for two gas pressures (0.084 and 0.133 kPa). Their overall uncertainty is quoted by Naidu et $al.$ to vary "between about $\pm5\%$ at the lowest E/N and about $\pm3\%$ at the high E/N values." These data are shown in Fig. 19. Although the data indicate a slight pressure dependence of D_T/μ (E/N), this variation is within the combined uncertainty of the measurements made at the two pressures. Thus, we performed a least squares fit to all the data in Fig. 19, which is shown by the solid line in the figure. Values from this fit are listed in Table 19 as the suggested data for the D_T/μ (E/N) of c-C$_4$F$_8$.

For measurements of D_T/μ (E/N) in two mixtures of c-C$_4$F$_8$ with Ar at relative concentrations of 0.468% and 4.91% see Yamaji et $al.$[94]

8. Ion–Molecule Reactions

There are three studies of ion–molecule reactions involving c-C$_4$F$_8$ which might be of interest to its use as a plasma processing gas. The first study is by Smith and Kevan[67] who
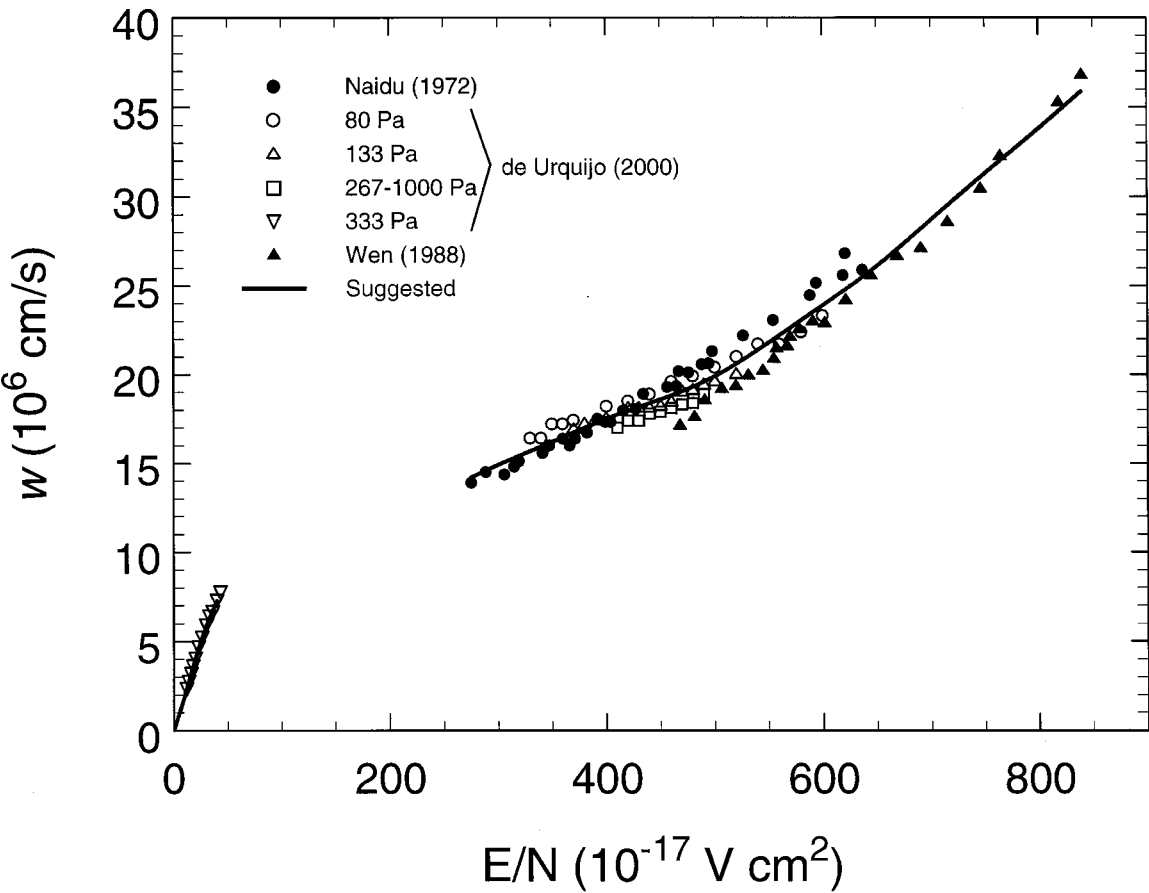

FIG. 17. Density-reduced electron attachment coefficient, η/N (E/N), for c-C$_4$F$_8$ (data of Naidu et $al.$[70]).

FIG. 18. Electron drift velocity, w (E/N), for c-C_4F_8 at room temperature: ($\bullet$) Ref. 70; ($\bigcirc$,$\triangle$,$\square$,$\triangledown$) Ref. 73; ($\blacktriangle$) Ref. 72; (—) suggested.

measured the cross sections for total and dissociative charge transfer in collisions of rare-gas positive ions with c-C_4F_8. They found that in such collisions the predominant ion is $C_2F_4^+$ at recombination energies of up to 16 eV. Only for Xe^+ bombardment did they detect a small parent positive ion c-$C_4F_8^+$. The second study is by Su and Kevan[95] on ion–molecule reactions in c-C_4F_8 using ICR mass spectrometry.

These studies have shown that fluoride transfer and collision-induced dissociation reactions predominate. The third study is by Morris et al.[96] who measured the rate constants and product branching ratios for reactions of the atmospheric ions O^+, O_2^+, O^-, O_2^-, NO^+, H_3O^+, CO_3^-, and NO_3^- with c-C_4F_8. They found that the last four ions are unreactive.

TABLE 18. Suggested room-temperature values of the electron drift velocity, w (E/N), for c-C_4F_8

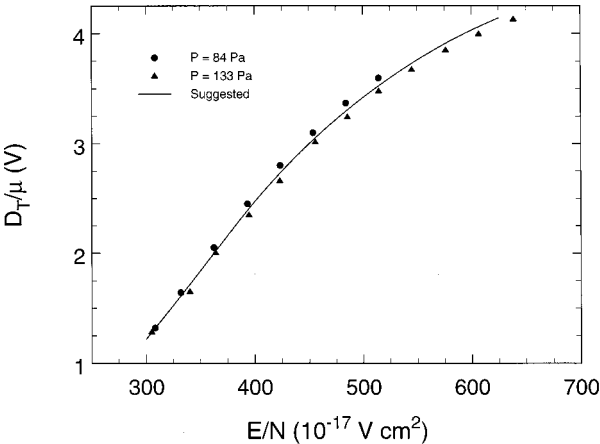| E/N $(10^{-17}$ V cm^2)	w (E/N) $(10^6$ cm s^{-1})	E/N $(10^{-17}$ V cm^2)	w (E/N) $(10^6$ cm s^{-1})
0	0.00	450	18.6
10	1.91	500	19.9
20	4.02	550	21.8
30	5.83	600	23.9
40	7.28	650	26.1
—	—	700	28.7
275	14.2	750	31.3
300	14.9	800	33.8
350	16.2	840	35.9
400	17.5		

FIG. 19. Ratio of the lateral electron diffusion coefficient to electron mobility, D_T/μ (E/N), for c-C_4F_8 $(T=293$ K) from Naidu et al.[70]

TABLE 19. Suggested values of D_T/μ (E/N) for c-C$_4$F$_8$ ($T=293$ K) derived from the data of Naidu *et al.*[70]

E/N (10^{-17} V cm^2)	D_T/μ (E/N) (V)
300	1.22
350	1.84
400	2.47
450	3.00
500	3.42
550	3.76
600	4.03
625	4.14

FIG. 20. Summary of suggested cross sections (see text).

9. Summary of Cross Sections and Rate Coefficients

The suggested values for the electron scattering cross sections of the c-C$_4$F$_8$ molecule are summarized in Fig. 20. These include values for

(i) $\sigma_{sc,t}(\varepsilon)$ from Fig. 2 and Table 4;
(ii) $\sigma_{i,t}(\varepsilon)$ from Fig. 6 and Table 9; and
(iii) $\sigma_{a,t}(\varepsilon)$ from Fig. 15(b) and Table 15

shown by the solid lines, and the lower-limit values of $\sigma_{dis,neu,t}(\varepsilon)$ from Fig. 9 and Table 11 shown by the broken line.

A number of additional electron collision cross sections have been discussed in this paper, and data on these can be found as follows:

(i) $\sigma_{e,diff}$ shown in Fig. 3 and Table 5;
(ii) $\sigma_{i,partial}(\varepsilon)$ shown in Fig. 5 and Tables 6 and 7; and
(iii) $\sigma_{dis,partial}(\varepsilon)$ shown in Fig. 9 and Table 11.

Based upon the discussions in this paper, recommended or suggested data for the electron transport coefficients, density-reduced electron attachment and ionization coefficients, and electron attachment rate constants have been presented as follows:

(i) $k_{a,t}(\langle\varepsilon\rangle)$ shown in Fig. 13 and Table 14;
(ii) w (E/N) shown in Fig. 18 and Table 18; and
(iii) D_T/μ (E/N) shown in Fig. 19 and Table 19.

10. Data Needs

The available data on both the electron collision cross sections and the electron transport coefficients are scarce and additional measurements and calculations are required. No determination of the momentum transfer and elastic integral cross sections are available, and cross sections for other si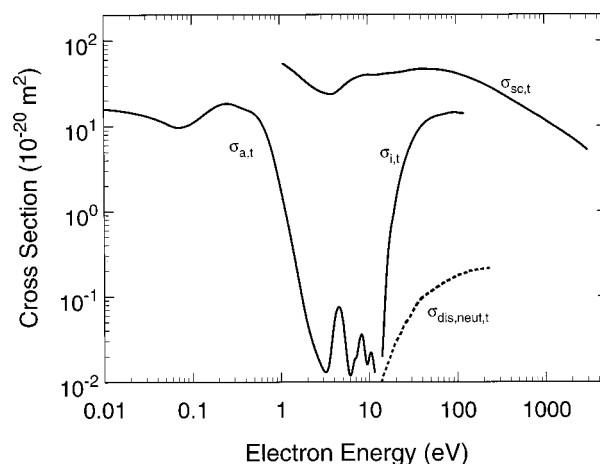gnificant low-energy electron collision processes such as vibrational and electronic excitation are also needed. Measurements of the electron transport coefficients over a wider range of values of the density-reduced electric field are also needed.

11. Acknowledgments

12. References

[1] J. W. Coburn, Plasma Chem. Plasma Process. **2**, 1 (1982).
[2] M. Miyamura, O. Tsukakoshi, and S. Komiya, J. Vac. Sci. Technol. **20**, 986 (1982).
[3] K. Nojiri and E. Iguchi, J. Vac. Sci. Technol. B **13**, 1451 (1995).
[4] T. Maruyama, N. Fujiwara, K. Shiozawa, and M. Yoneda, J. Vac. Sci. Technol. A **13**, 810 (1995).
[5] H. Kimura, K. Shiozawa, K. Kawai, H. Miyatake, and M. Yoneda, Jpn. J. Appl. Phys., Part 1 **34**, 2114 (1995).
[6] K. Miyata, M. Hori, and T. Goto, Jpn. J. Appl. Phys., Part 1 **36**, 5340 (1997).
[7] S. Samukawa and T. Mukai, Proceedings of the International Symposium on Electron-Molecule Collisions and Swarms, edited by Y. Hatano, H. Tanaka, and N. Kouchi, 18-20 Tokyo, Japan, July, 1999, p. 76.
[8] J. N. Butler, J. Am. Chem. Soc. **84**, 1393 (1962).
[9] J. M. Simmie, W. J. Quiring, and E. Tschuikow-Roux, J. Phys. Chem. **73**, 3830 (1969).
[10] J. M. Preses, R. E. Weston, Jr., and G. W. Flynn, Chem. Phys. Lett. **46**, 69 (1977).
[11] M. Quack and G. Seyfang, Ber. Bunsenges. Phys. Chem. **86**, 504 (1982).
[12] E. Pochon, R. E. Weston, Jr., and G. W. Flynn, J. Phys. Chem. **89**, 86 (1985).
[13] A. Yokoyama, K. Yokoyama, and G. Fujisawa, Chem Phys. Lett. **237**, 106 (1995).
[14] E. W. D. Norton, Trans. Am. Acad. Ophalmol. Otolaryngol. **77**, 85 (1973).

[15] S. Brubaker, G. A. Peyman, and C. Vygantas, Arch. Ophthalmol. **92**, 324 (1974).

[16] L. G. Christophorou, R. A. Mathis, D. R. James, and D. L. McCorkle, J. Phys. D **14**, 1889 (1981).

[17] L. G. Christophorou, D. R. James, and R. A. Mathis, J. Phys. D **14**, 675 (1981).

[18] L. G. Christophorou, R. A. Mathis, S. R. Hunter, and J. G. Carter, J. Appl. Phys. **63**, 52 (1988).

[19] L. G. Christophorou, Nucl. Instrum. Methods Phys. Res. A **268**, 424 (1988).

[20] J. T. Houghton, L. G. M. Filho, B. A. Callander, N. Harris, A. Kattenberg, and K. Maskell, *Climate Change 1995* (Cambridge University Press, New York, 1996), p. 22.

[21] R. A. Morris, T. M. Miller, A. A. Viggiano, J. F. Paulson, S. Solomon, and G. Reid, J. Geophys. Res. **100**, 1287 (1995).

[22] L. G. Christophorou, J. K. Olthoff, and M. V. V. S. Rao, J. Phys. Chem. Ref. Data **25**, 1341 (1996).

[23] L. G. Christophorou, J. K. Olthoff, and M. V. V. S. Rao, J. Phys. Chem. Ref. Data **26**, 1 (1997).

[24] L. G. Christophorou, J. K. Olthoff, and Y. Wang, J. Phys. Chem. Ref. Data **26**, 1205 (1997).

[25] L. G. Christophorou and J. K. Olthoff, J. Phys. Chem. Ref. Data **27**, 1 (1998).

[26] L. G. Christophorou and J. K. Olthoff, J. Phys. Chem. Ref. Data **27**, 889 (1998).

[27] L. G. Christophorou and J. K. Olthoff, J. Phys. Chem. Ref. Data **28**, 131 (1999).

[28] L. G. Christophorou and J. K. Olthoff, J. Phys. Chem. Ref. Data **28**, 967 (1999).

[29] L. G. Christophorou and J. K. Olthoff, J. Phys. Chem. Ref. Data **29**, 267 (2000).

[30] L. G. Christophorou and J. K. Olthoff, J. Phys. Chem. Ref. Data **29**, 553 (2000).

[31] J. P. Novak and M. F. Fréchette, J. Appl. Phys. **63**, 2570 (1988).

[32] H. Itoh, T. Miyachi, M. Kawaguchi, Y. Nakao, and H. Tagashira, J. Phys. D **24**, 277 (1991).

[33] O. Bastiansen, O. Hassel, and L. K. Lund, Acta Chem. Scand. **3**, 297 (1949).

[34] H. P. Lemaire and R. L. Livingston, J. Am. Chem. Soc. **74**, 5732 (1952).

[35] N. V. Alekseev, I. A. Ronova, and P. P. Barzdain, Zh. Strukt. Khim. **9**, 1073 (1968).

[36] C. H. Chang, R. F. Porter, and S. H. Bauer, J. Mol. Struct. **7**, 89 (1971).

[37] N. V. Alekseev and P. P. Barzdain, Zh. Strukt. Khim. **15**, 181 (1972).

[38] B. Beagley, R. Calladine, R. G. Pritchard, and S. F. Taylor, J. Mol. Struct. **158**, 309 (1987).

[39] R. P. Bauman and B. J. Bulkin, J. Chem. Phys. **45**, 496 (1966).

[40] F. A. Miller and R. J. Capwell, Spectrochim. Acta **27A**, 1113 (1971).

[41] C. Mao, C.-S. Nie, and Z.-Y. Zhu, Spectrochim. Acta **44A**, 1093 (1988).

[42] G. Fischer, R. L. Purchase, and D. M. Smith, J. Mol. Struct. **405**, 159 (1997).

[43] T. M. Miller, R. A. Morris, A. E. S. Miller, A. A. Viggiano, and J. F. Paulson, Int. J. Mass Spectrom. Ion Processes **135**, 195 (1994).

[44] K. G. Mothes and R. N. Schindler, Ber. Bunsenges. Phys. Chem. **75**, 938 (1971).

[45] C. Lifshitz, T. O. Tiernan, and B. M. Hughes, J. Chem. Phys. **59**, 3182 (1973).

[46] G. K. Jarvis, K. J. Boyle, C. A. Mayhew, and R. P. Tuckett, J. Phys. Chem. A **102**, 3230 (1998).

[47] C. Lifshitz and R. Grajower, Int. J. Mass Spectrom. Ion Phys. **10**, 25 (1972/1973).

[48] M. B. Robin, *Higher Excited States of Polyatomic Molecules* (Academic, New York, 1974), Vol. I, p. 180.

[49] M. M. Bibby and G. Carter, Trans. Faraday Soc. **59**, 2455 (1963).

[50] L. Kevan and J. H. Futrell, J. Chem. Soc., Faraday Trans. II **68**, 1742 (1972).

[51] I. Sauers, L. G. Christophorou, and J. G. Carter, J. Chem. Phys. **71**, 3016 (1979).

[52] R. Grajower and C. Lifshitz, Israel J. Chem. **6**, 847 (1968).

[53] M. V. Kurepa, 3rd Cz. Conference on Electronics and Vacuum Physics Transactions, 1965, p. 107.

[54] P. W. Harland and J. C. J. Thynne, Int. J. Mass Spectrom. Ion Phys. **10**, 11 (1972/1973).

[55] P. W. Harland and J. L. Franklin, J. Chem. Phys. **61**, 1621 (1974).

[56] I. Ishii, R. McLaren, A. P. Hitchcock, K. D. Jordan, Y. Choi, and M. B. Robin, Can. J. Chem. **66**, 2104 (1988).

[57] J. E. Sanabia, G. D. Cooper, J. A. Tossell, and J. H. Moore, J. Chem. Phys. **108**, 389 (1998).

[58] H. Nishimura, Proceedings of the International Symposium on Electron-Molecule Collisions and Swarms, edited by Y. Hatano, H. Tanaka, and N. Kouchi, Tokyo, Japan, 18–20 July, 1999, p. 103.

[59] H. Nishimura (private communication, November 1999).

[60] M. Okamoto, M. Hoshino, Y. Sakamoto, S. Watanabe, M. Kitajima, H. Tanaka, and M. Kimura, Proceedings of the International Symposium on Electron-Molecule Collisions and Swarms, edited by Y. Hatano, H. Tanaka, and N. Kouchi, Tokyo, Japan, 18–20 July, 1999, p. 191.

[61] H. Tanaka (private communication, 2000).

[62] V. McKoy, as quoted in Ref. 61; C. Winstead and V. McKoy, J. Chem. Phys. **114**, 7407 (2001).

[63] H. Toyoda, M. Ito, and H. Sugai, Jpn. J. Appl. Phys. **36**, 3730 (1997).

[64] C. Q. Jiao, A. Garscadden, and P. D. Haaland, in *Gaseous Dielectrics VIII*, edited by L. G. Christophorou and J. K. Olthoff (Kluwer Academic/Plenum, New York, 1998), p. 57.

[65] C. Q. Jiao, A. Garscadden, and P. D. Haaland, Chem. Phys. Lett. **297**, 121 (1998).

[66] R. C. Wetzel, F. A. Baioochi, T. R. Hayes, and R. S. Freund, Phys. Rev. **35**, 559 (1997).

[67] D. L. Smith and L. Kevan, J. Chem. Phys. **55**, 2290 (1971).

[68] J. A. Beran and L. Kevan, J. Phys. Chem. **73**, 3866 (1969).

[69] V. Tarnovsky and K. Becker, J. Chem. Phys. **98**, 7868 (1993).

[70] M. S. Naidu, A. N. Prasad, and J. D. Craggs, J. Phys. D **5**, 741 (1972).

[71] T. Tagashira, Y. Miyamoto, and M. Shimozuma, Proceedings of the XVIII International Conference on Phenomena in Ionized Gases, Swansea, U. K., 13–17 July, 1987, p. 680.

[72] C. Wen and J. M. Wetzer, IX International Conference on Gas Discharges and their Applications, Venezia, Italy, 19–23 September, 1988, p. 367.

[73] J. de Urquijo (private communication, July 2000); J. de Urquijo and E. Basurto, J. Phys. D **34**, 1352 (2001).

[74] J. Berril, M. J. Christensen, and I. W. McAllister, in *Gaseous Dielectrics V*, edited by L. G. Christophorou and D. W. Bouldin (Pergamon, New York, 1987), p. 304.

[75] L. G. Christophorou, R. A. Mathis, S. R. Hunter, and J. G. Carter, in *Gaseous Dielectrics V*, edited by L. G. Christophorou and D. W. Bouldin (Pergamon, New York, 1987), p. 88.

[76] H. Kazumi, R. Hamasaki, and K. Tago, Plasma Sources Sci. Technol. **5**, 200 (1996).

[77] L. G. Christophorou, D. L. McCorkle, and A. A. Christodoulides, in *Electron-Molecule Interactions and Their Applications*, edited by L. G. Christophorou (Academic, New York, 1984), Vol. 1, Chap. 6.

[78] W. T. Naff, C. D. Cooper, and R. N. Compton, J. Chem. Phys. **49**, 2784 (1968).

[79] J. M. S. Henis and C. A. Mabie, J. Chem. Phys. **53**, 2999 (1970).

[80] R. L. Woodin, M. S. Foster, and J. L. Beauchamp, J. Chem. Phys. **72**, 4223 (1980).

[81] L. G. Christophorou, Adv. Electron. Electron Phys. **46**, 55 (1978).

[82] A. Chutjian and S. H. Alajajian, J. Phys. B **20**, 839 (1987).

[83] A. A. Christodoulides, L. G. Christophorou, R. Y. Pai, and C. M. Tung, J. Chem. Phys. **70**, 1156 (1979).

[84] R. M. Reese, V. H. Dibeler, and F. L. Mohler, J. Res. Nat. Bur. Stand. **57**, 367 (1956).

[85] A. Kono and K. Kato, Appl. Phys. Lett. **77**, 495 (2000).

[86] S. M. Spyrou, S. R. Hunter, and L. G. Christophorou, J. Chem. Phys. **83**, 641 (1985).

[87] L. G. Christophorou, D. L. McCorkle, and D. Pittman, J. Chem. Phys. **60**, 1183 (1974).

[88] A. A. Christodoulides, L. G. Christophorou, and D. L. McCorkle, Chem. Phys. Lett. **139**, 350 (1987).

[89] E. Schultes, Ph.D. dissertation, University of Bonn, 1973; as quoted in Ref. 90.

[90] A. A. Christodoulides, E. Schultes, R. Schumacher, and R. N. Schindler, Z. Naturforsch. **29a**, 389 (1974).

[91] F. J. Davis, R. N. Compton, and D. R. Nelson, J. Chem. Phys. **59**, 2324 (1973).

[92] K. M. Bansal and R. W. Fessenden, J. Chem. Phys. **59**, 1760 (1973).

[93] L. G. Christophorou and P. G. Datskos, Int. J. Mass Spectrom. Ion Processes **149/150**, 59 (1995).

[94] M. Yamaji, Y. Okada, and Y. Nakamura, Proceedings of the International Symposium on Electron-Molecule Collisions and Swarms, edited by Y.

Hatano, H. Tanaka, and N. Kouchi, Tokyo, Japan, 18–20 July 1999, p. 151.

[95] T. Su and L. Kevan, J. Phys. Chem. **77**, 148 (1973).

[96] R. A. Morris, A. A. Viggiano, S. T. Arnold, and J. F. Paulson, Int. J. Mass Spectrom. Ion Processes **149/150**, 287 (1995).